Electronic Supplementary Material (ESI) for Organic & Biomolecular Chemistry.
This journal is © The Royal Society of Chemistry 2015

Supporting Information

New PKS-NRPS tetramic acids and pyridinone from an Australian marine-derived fungus, *Chaunopycnis* sp.

Zhuo Shang,[a] Li Li,[c] Breno P. Espósito,[d] Angela A. Salim,[a] Zeinab G. Khalil,[a] Michelle Quezada,[a] Paul V. Bernhardt[b] and Robert J. Capon[a]*

[a]Institute for Molecular Bioscience, The University of Queensland, St Lucia, Queensland 4072, Australia

[b]School of Chemistry and Molecular Biosciences, The University of Queensland, St Lucia, Queensland 4072, Australia

[c]Beijing Key Laboratory of Active Substances Discovery and Druggability Evaluation, Institute of Materia Medica, Chinese Academy of Medical Sciences & Peking Union Medical College, Beijing 100050, China

[d]Institute of Chemistry, University of São Paulo, 05508-000, São Paulo, Brazil

Table of Contents

1 General experimental procedures

Specific optical rotations ($[\alpha]_D$) were measured on a JASCO P-1010 polarimeter in a 100 × 2 mm cell at 22 °C. UV-vis spectra were obtained on a Varian Cary 50 UV-visible spectrophotometer with 1 cm pathway quartz cells. CD spectra were recorded at 22 °C on a JASCO J-810 spectropolarimeter. Optical density (OD) and fluorescence of 96-well microtitre plates were measured at room temperature on a POLARstar Omega microtitre plate reader. NMR spectra were acquired on a Bruker Avance 600 MHz spectrometer and referenced to residual solvent proton and carbon signals of the deuterated solvent. ESIMS experiments were carried out on an Agilent 1100 series LC/MSD (single quadrupole) instrument. High-resolution ESIMS spectra were obtained on a Bruker micrOTOF mass spectrometer by direct infusion in MeCN at 3 μL/min using sodium formate clusters as an internal calibrant. Liquid chromatography-diode array-mass spectrometry (LC-DAD-MS) data were acquired on an Agilent 1100 series separation module equipped with an Agilent 1100 series LC/MSD mass detector and diode array multiple wavelength detector. Semi-preparative HPLC was performed using Agilent 1100 series LC instruments with corresponding detectors, fraction collectors and software inclusively. Pure compounds eluting from semi-preparative HPLC were dried on a Christ freeze dryer. Microorganisms were manipulated under sterile conditions provided by a Laftech class II biological safety cabinet and incubated in MMM Friocell incubators or Innova 42 incubator shakers with temperature set at 26.5 °C. NMR chemical shift calculation and MM2 energy minimization were carried out on ACD/Labs 7.0 and ChemBio3D Ultra 13.0 software, respectively.

2 Fungal strain taxonomy

Fungus CMB-MF028 formed circular white colonies with fan-shaped wrinkles and no spores on peptone yeast glucose (PYG) agar and ISP-2 agar plates. Genomic DNA from this isolate was extracted from the mycelia using the DNeasy Plant Mini Kit (Qiagen) as per the manufacturers protocol. The rRNA genes were amplified by PCR using the universal primers ITS 1 (5″-TCCGTAGGTGAACCTGCGG-3″) and ITS 4 (5″-TCCTCCGCTTATTGATATGC-3″) purchased from Sigma-Aldrich. The PCR mixture (50 μL) contained genomic DNA (1 μL, 20–40 ng), four deoxynucleoside triphosphates (dNTP, 200 μM each), $MgCl_2$ (1.5 mM), primer (0.3 μM each), 1 U of *Taq* DNA polymerase (Fisher Biotec) and PCR buffer (5 μL, 10×). PCR was performed using the following conditions: initial denaturation at 95 °C for 3 min, 30 cycles in series of 94 °C for 30 s (denaturation), 55 °C for 60 s (annealing) and 72 °C for 60 s (extension), followed by one cycle at 72 °C for 6 min. The PCR products were purified with PCR purification kit (Qiagen) and sequenced. The BLAST search showed the amplified ITS sequence (GenBank accession no. KP881722) has

98% homology with other members of the genus *Chaunopycnis* sp.

ITS gene sequence of CMB-MF028

GGGATCCGAGCTACACTCCCAACCCCTGTGACATACCCGAACGTTGCCTCGGCG
GGACCGCCCCGGCGCCCACAGCGGCCCGGAACCAGGCGCCCGCCGGAGGACCC
AAACTCTTGCTTTAAACAGTGGCATACTCTCTGAGTCTCACAAACAAAAAATAA
ATCAAAACTTTCAACAACGGATCTCTTGGCTCTGGCATCGATGAAGAACGCAGC
GAAATGCGATAAGTAATGTGAATTGCAGAATTCAGTGAATCATCGAATCTTTGA
ACGCACATTGCGCCCGCCAGCATTCTGGCGGGCATGCCTGTCCGAGCGTCATTT
CAACCCTCAGGGAGCCCCCTCGCGGGGGGGGATGGCGGGTTGGGGGCCGGCCGC
CCAGCGCGCGCCGCCCCCGAAATGCAGTGGCGACCTCGCCGCAGCCTCCCCTGC
GTAGTAGCACAACCTCGCACCGGAGCGCGGAGACGGTCACGCCGTAAAACGCCC
CAACTTTCAAGAGTTGACCTCGGATCAG (511 bp)

BLAST search (closest match)

Chaunopycnis alba internal transcribed spacer 1, 5.8S ribosomal RNA gene and internal transcribed spacer 2, complete sequence; and 28S ribosomal RNA gene, partial sequence

Sequence ID: gb|AF389192.1|AF389192 Length: 510 Number of Matches: 1

Related Information

Range 1: 12 to 510 GenBank Graphics ▼ Next Match ▲ Previous Match

Score	Expect	Identities	Gaps	Strand
859 bits(465)	0.0	488/499(98%)	2/499(0%)	Plus/Plus

```
Query  15   ACTCCC-AACCCCTGTG-ACATACCCGAACGTTGCCTCGGCGGGACCGCCCCGGCGCCCA  72
            ||||||  |||||||||| |||||||||||||||||||||||||||||||||||||||||
Sbjct  12   ACTCCCAAACCCCTGTGAACATACCCGAACGTTGCCTCGGCGGGACCGCCCCGGCGCCCC  71

Query  73   CAGCGGCCCCGGAACCAGGCGCCCGCCGGAGGACCCAAACTCTTGCTTTAAACAGTGGCAT  132
            ||||||||||||||||||||||||||||||||||||||||||||||||||||||||||||||
Sbjct  72   TAGCGGCCCCGGAACCAGGCGCCCGCCGGAGGACCCAAACTCTTGCTTTAAACAGTGGCAT  131

Query  133  ACTCTCTGAGTCTCACAAACAAAAAATAAATCAAAACTTTCAACAACGGATCTCTTGGCT  192
            ||||||||||||||||||||||||||||||||||||||||||||||||||||||||||||||
Sbjct  132  ACTCTCTGAGTCTCACAAACAAAAAATAAATCAAAACTTTCAACAACGGATCTCTTGGCT  191

Query  193  CTGGCATCGATGAAGAACGCAGCGAAATGCGATAAGTAATGTGAATTGCAGAATTCAGTG  252
            ||||||||||||||||||||||||||||||||||||||||||||||||||||||||||||||
Sbjct  192  CTGGCATCGATGAAGAACGCAGCGAAATGCGATAAGTAATGTGAATTGCAGAATTCAGTG  251

Query  253  AATCATCGAATCTTTGAACGCACATTGCGCCCGCCAGCATTCTGGCGGGCATGCCTGTCC  312
            ||||||||||||||||||||||||||||||||||||||||||||||||||||||||||||||
Sbjct  252  AATCATCGAATCTTTGAACGCACATTGCGCCCGCCAGCATTCTGGCGGGCATGCCTGTCC  311

Query  313  GAGCGTCATTTCAACCCTCAGGGAGCCCCCTCGCgggggggATGGCGGGTTGGGGGCCGG  372
            |||||||||||||||||||||| |||||| ||||||||||     |||||||||||||
Sbjct  312  GAGCGTCATTTCAACCCTCAGGGAACCCCCTTGCGGGGGGGGACCTGGTGTTGGGGGCCGG  371

Query  373  CCGCCCAGCGCGCGCCGCCCCCGAAATGCAGTGGCGACCTCGCCGCAGCCTCCCCTGCGT  432
            ||||||||||||||||||||||||||||||||||||||||||||||||||||||||||||||
Sbjct  372  CCGCCCAGCGCGCGCCGCCCCCGAAATGCAGTGGCGACCTCGCCGCAGCCTCCCCTGCGT  431

Query  433  AGTAGCACAACCTCGCACCGGAGCGCGGAGACGGTCACGCCGTAAAACGCCCAACTTTCA  492
            ||||||||||||||||||||||||||||||||||||||||||||||||||||||||||||||
Sbjct  432  AGTAGCACAACCTCGCACCGGAGCGCGGAGACGGTCACGCCGTAAAACGCCCAACTTTCA  491

Query  493  AGAGTTGACCTCGGATCAG  511
            ||||||||||||||||||
Sbjct  492  AGAGTTGACCTCGGATCAG  510
```

Chaunopycnis alba internal transcribed spacer 1, 5.8S ribosomal RNA gene and internal transcribed spacer 2, complete sequence; and 28S ribosomal RNA gene, partial sequence

GenBank: AF389192.1

FASTA Graphics PopSet

Go to:

```
LOCUS       AF389192                510 bp    DNA     linear   PLN 15-JUL-2001
DEFINITION  Chaunopycnis alba internal transcribed spacer 1, 5.8S ribosomal RNA
            gene and internal transcribed spacer 2, complete sequence; and 28S
            ribosomal RNA gene, partial sequence.
ACCESSION   AF389192
VERSION     AF389192.1  GI:14718633
KEYWORDS    .
SOURCE      Chaunopycnis alba
  ORGANISM  Chaunopycnis alba
            Eukaryota; Fungi; Dikarya; Ascomycota; Pezizomycotina;
            Sordariomycetes; Hypocreomycetidae; Hypocreales; Clavicipitaceae;
            mitosporic Clavicipitaceae; Chaunopycnis.
REFERENCE   1  (bases 1 to 510)
  AUTHORS   Bills,G.F., Polishook,J.D., Goetz,M.A., Sullivan,R.F. and
            White,J.F. Jr.
  TITLE     Chaunopycnis pustulata sp. nov., a new clavicipitalean anamorph
            producing metabolites that modulate potassium ion channels
  JOURNAL   Unpublished
REFERENCE   2  (bases 1 to 510)
  AUTHORS   Bills,G.F., Polishook,J.D., Goetz,M.A., Sullivan,R.F. and
            White,J.F. Jr.
  TITLE     Direct Submission
  JOURNAL   Submitted (07-JUN-2001) Natural Products Drug Discovery, Merck
            Research Laboratories, P.O. Box 2000, Rahway, NJ 07065, USA
```

3 Bioassays

Antimicrobial assay. Antimicrobial activities were measured against Gram-positive bacteria *Staphylococcus aureus* (ATCC 25923), *Staphylococcus epidermidis* (ATCC 12228) and *Bacillus subtilis* (ATCC 6633)), Gram-negative bacteria *Escherichia coli* (ATCC 25922), *Pseudomonas aeruginosa* (ATCC 27853) and *Klebsiella pneumonia* (ATCC 13883), and a fungus *Candida albicans* (ATCC 90028) by the broth micro-dilution method. The test was performed (in triplicate) in 96-well microtiter plates by serial dilution in tryptic soy broth for bacteria and Sabouraud broth for fungi, respectively. Test compounds were prepared and serially (ten-fold) diluted in 10% DMSO. An aliquot (20 μL) of each dilution was transferred to a 96-well microtiter plate, followed by freshly prepared microbial broth (180 μL, 10^4–10^5 cfu/mL cell density) to give a final test compound concentration ranging from 32 to 0.125 μg/mL. The plates were incubated at 37 °C for 24 h for bacteria and at 26.5 °C for 48 h for yeast. The optical density of each well was measured at 600 nm using a microtitre plate spectrophotometer (POLARstar Omega plate, BMG LABTECH, Offenburg, Germany). Broth medium with and without microbial inoculation were used as negative controls, with tetracycline and ketoconazole used as positive controls for antibacterial and antifungal assays, respectively. The minimum inhibitory concentration (MIC, μg/mL) was determined as the lowest concentration of a test compound that inhibits 90% of microorganism growth. In addition, IC_{50} values (μM) were calculated using Prism 5.0 (GraphPad Software Inc., La Jolla, CA), as the concentration of compound required for 50% inhibition of bacterial growth.

Cytotoxicity assay. The MTT (3-(4,5-dimethylthiazol-2-yl)-2,5-diphenyltetrazolium bromide) assay was modified from that previously described[1] using adherent NCIH460 (human large cell lung carcinoma), SW620 (human colorectal adenocarcinoma) and KB3-1 (human cervical carcinoma) cell lines. Briefly, cells were harvested with trypsin and dispensed into 96-well microtitre assay plates at 2,000 cells/well and incubated for 18 h at 37 °C with 5% CO_2 (to allow cells to attach). Compounds were dissolved in 5% DMSO in PBS (*v*/*v*) and aliquots (20 μL) were tested over a series of final concentrations ranging from 10 nM to 30 μM. Vinblastine was used as positive control and blank control wells were treated with 5% aqueous DMSO. After 68 h incubation at 37 °C with 5% CO_2, an aliquot (20 μL) of MTT in PBS (4 mg/mL) was added to each well (final concentration of 0.4 mg/mL), and the microtitre plates incubated for a further 4 h at 37 °C with 5% CO_2. After this final incubation the medium was aspirated and precipitated formazan crystals dissolved in DMSO (100 μL/well). The absorbance of each well was measured at $OD_{580\ nm}$ at r.t. on a POLARstar Omega microtitre plate reader. IC_{50} values were calculated using Prism 5.0

(GraphPad Software Inc., La Jolla, CA), as the concentration of analyte required for 50% inhibition of cancer cell growth (compared to negative controls). All experiments were performed in duplicate.

***Calcein-Fe (CAFe)* Assay.** Analytes **1**–**6** were prepared and serially diluted in DMSO, and an aliquot (5 μL) of each dilution was dispensed into 96-well flat microtiter plates in duplicate. An aliquot (95 μL) of 2 μM calcein-Fe complex (CAFe) in HBS:DMSO (50:50, *v*/*v*) was then dispensed into each well to give a final analyte concentration ranging from 0 to 50 μM. HBS (Hepes Buffered Saline) was prepared by dissolving HEPES (20 mM) and NaCl (150 mM) in distilled H_2O, washed with Chelex(R)-100 (0.01 g/mL) and finally adjusted pH to 7.4. CAFe was prepared by dissolving $FeSO_4$ in aqueous calcein in order to reach a final concentration of 10 mM in both Fe and calcein. Assay plates were incubated at r.t. in the dark overnight, after which the fluorescence of each well was measured at r.t. using a POLARstar Omega microtitre plate reader (top reading; $\lambda_{exc}/\lambda_{em}$ = 485/530 nm; gain 850). A calibration curve was generated using desferrioxamine (DFO) (0 to 2 μM) as the positive control. The apparent binding constant (K_{app}) was calculated from the following equation[2]

$$K_{app} = \frac{[CA][Fe(chelator)_3]}{[CAFe][chelator]^3 K_{diss(CAFe)}}$$

where $K_{diss(CAFe)} = 1.0\times10^{-24}$.

***Metal ion chelating assay*.** Analytes (15 μg) were dissolved in metal salt solutions (20 μL) consisting of either 4 mol equivalent of $FeCl_3$, $FeSO_4$, $CuSO_4$, $AlCl_3$ or $ZnSO_4$ in MeOH, or 4 mol equivalent of $MgSO_4$ in 70% aqueous MeOH, and the solutions shaken at r.t. for 2 d. The resulting solutions were diluted with MeOH (to 1 mL) and their UV-vis spectra were measured (200-600 nm), after which the solutions were dried under nitrogen, re-dissolved in MeOH (40 μL), and subjected to HRESI(±)MS analysis to detect the presence of metal chelated pseudo-molecular ions.

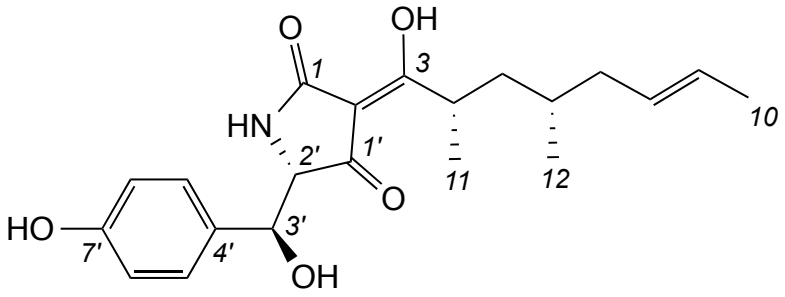

Table S1. NMR (600 MHz, DMSO-d_6) data for F-14329 (**1**)

Pos.	δ_H (mult., J (Hz))	δ_C	COSY	HMBC (^{1}H to ^{13}C)
1	–	176.0	–	–
2	–	100.6	–	–
3	–	191.5	–	–
4	3.49 (br m)	33.4	5a, 5b, 11	5, 11
5a	1.62 (m)[b]	39.8[d]	4, 5b, 6	6, 7, 12
5b	1.04 (m)		4, 5a, 6	6, 12
6	1.24 (m)	30.8	5a, 5b, 7a, 7b, 12	–
7a	1.86 (m)	39.9[d]	6, 7b, 8	5, 6, 8, 9, 12
7b	1.74 (m)		6, 7a, 8	5, 6, 8, 9, 12
8	5.33 (m)[a]	129.3[c]	7a, 7b, 9	7, 9, 10
9	5.34 (m)[a]	125.9	8, 10	7, 8, 10
10	1.59 (d, 5.2)[b]	17.8	9	8, 9
11	0.88 (d, 6.3)	18.1	4	3, 4, 5
12	0.77 (d, 6.3)	19.1	6	6, 7
1’	–	192.6	–	–
2’	4.16 (br s)	68.0	3’, -NH	1, 1’, 3’, 4’
3’	4.87 (br s)	72.6	2’, 5’/9’	1’, 2’, 5’/9’
4’	–	129.3[c]	–	–
5’/9’	7.00 (d, 8.5)	128.2	3’, 6’/8’	3’, 5’/9’, 6’/8’, 7’
6’/8’	6.59 (d, 8.5)	114.1	5’/9’	4’, 5’/9’, 6’/8’, 7’
7’	–	156.5	–	–
3’-OH	5.65 (br s)	–	–	–
7’-OH	9.23 (br s)	–	–	–
-NH	9.14 (br s)	–	2’	2, 1’, 2’

[a, b, c] Overlapping signals; [d] Overlapped with residual DMSO signal.
Only one set of signal was observed in DMSO-d_6.

Table S2. NMR (600 MHz, $CDCl_3$) data for F-14329 (**1**)

Pos.	F-14329 (**1**)[d]			
	Exo-enolic form A (major)		*Exo*-enolic form B (minor)	
	δ_H (mult., *J* (Hz))	δ_C	δ_H (mult., *J* (Hz))	δ_C
1	–	175.7	–	169.2
2	–	100.5	–	104.1
3	–	194.6	–	196.0
4	3.70 (m)	34.4	3.69 (m)	33.7
5a	1.78 (m)[b]	40.4[c]	1.73 (m)[b]	40.5[c]
5b	1.17 (m)		1.08 (m)	
6	1.35 (m)	31.4	1.35 (m)	31.3
7a	1.96 (m)	40.4[c]	1.86 (m)	40.5[c]
7b	1.80 (m)[b]		1.76 (m)[b]	
8	5.34 (m)[a]	129.3	5.34 (m)[a]	129.5
9	5.39 (m)[a]	126.7	5.39 (m)[a]	126.5
10	1.64 (d, 6.0)	18.1	1.64 (d, 6.1)	18.7
11	1.11 (d, 6.7)	18.5	1.14 (d, 6.7)	19.1
12	0.86 (d, 6.7)	19.6	0.70 (d, 6.4)	19.4
1’	–	194.7	–	201.2
2’	3.99 (d, 7.3)	65.9	4.25 (d, 5.4)	64.3
3’	4.76 (d, 7.3)	74.3	4.93 (d, 5.4)	74.1
4’	–	129.9	–	129.2
5’/9’	7.16 (d, 8.0)	128.5	7.08 (d, 8.0)	128.3
6’/8’	6.71 (d, 8.0)	115.7	6.58 (d, 8.0)	115.5
7’	–	156.7	–	156.7
3’-OH	–	–	–	–
7’-OH	–	–	–	–
-NH	6.10 (br s)	–	6.14 (br s)	–

[a, b, c] Overlapping signals; [d] The ratio of *Exo*-enolic form A and B of **1** is approximately 5:1 in $CDCl_3$

Table S3. Differences of NMR (600 MHz, $CDCl_3$) data for two tautomers of F-14329 (**1**)

Pos.	$\delta_{H\ (Exo\ A)} - \delta_{H\ (Exo\ B)}$	$\delta_{C\ (Exo\ A)} - \delta_{C\ (Exo\ B)}$
1	–	+6.5
2	–	–3.6
3	–	–1.4
4	+0.01	+0.7
5a	+0.05	–0.1
5b	+0.09	–
6	0	+0.1
7a	+0.1	–0.1
7b	+0.04	–
8	0	–0.2
9	0	+0.2
10	0	-0.2
11	–0.03	–1.0
12	+0.16	+0.2
1’	–	–6.5
2’	–0.26	+1.6
3’	–0.17	+0.2
4’	–	+0.7
5’/9’	+0.08	+0.2
6’/8’	+0.13	+0.2
7’	–	0

Table S4. Comparison of NMR ($CDCl_3$) data for **1** and the patented F-14329[3]

Pos.	**1**[d]				F-14329[3]			
	Exo-enolic form A (major)		*Exo*-enolic form B (minor)		*Exo*-enolic form A (major)		*Exo*-enolic form B (minor)	
	δ_H (mult., *J* (Hz))	δ_C	δ_H (mult., *J* (Hz))	δ_C	δ_H (mult., *J* (Hz))	δ_C	δ_H (mult., *J* (Hz))	δ_C
1	–	175.7	–	169.2	–	175.7	–	169.9
2	–	100.5	–	104.1	–	100.5	–	104.1
3	–	194.6	–	196.0	–	194.4	–	195.8
4	3.70 (m)	34.4	3.69 (m)	33.7	3.65 (m)	34.1	3.65 (m)	33.6
5α	1.78 (m)[b]	40.4[c]	1.73 (m)[b]	40.5[c]	1.77 (m)	40.1	1.77 (m)	40.2
5β	1.17 (m)		1.08 (m)		1.13 (m)		1.11 (d, 6.4)	
6	1.35 (m)	31.4	1.35 (m)	31.3	1.33 (d, 5.4)	31.3	1.33 (d, 5.4)	31.1
7α	1.96 (m)	40.4[c]	1.86 (m)	40.5[c]	1.95 (m)	40.2	1.95 (m)	40.4
7β	1.80 (m)[b]		1.76 (m)[b]					
8	5.34 (m)[a]	129.3	5.34 (m)[a]	129.5	5.37 (m)	129.1	5.37 (m)	129.3
9	5.39 (m)[a]	126.7	5.39 (m)[a]	126.5	5.39 (m)	126.6	5.39 (m)	126.4
10	1.64 (d, 6.0)	18.5	1.64 (d, 6.1)	18.7	1.64 (d, 5.4)	18.3	1.64 (d, 5.4)	18.0
11	1.11 (d, 6.7)	18.1	1.14 (d, 6.7)	19.1	1.04 (d, 6.4)	18.0	1.16 (d, 8.3)	18.6
12	0.86 (d, 6.7)	19.6	0.70 (d, 6.4)	19.4	0.84 (d, 6.4)	19.4	0.61 (d, 5.9)	19.2
1’	–	194.7	–	201.2	–	194.2	–	200.6
2’	3.99 (d, 7.3)	65.9	4.25 (d, 5.4)	64.3	4.03 (d, 5.4)	66.1	4.25 (br s)	64.3
3’	4.76 (d, 7.3)	74.3	4.93 (d, 5.4)	74.1	4.81 (d, 5.4)	74.0	4.95 (br s)	73.9
4’	–	129.9	–	129.2	–	129.3	–	128.6
5’/9’	7.16 (d, 8.0)	128.5	7.08 (d, 8.0)	128.3	7.07 (d, 7.3)	128.5	7.00 (br s)	128.2
6’/8’	6.71 (d, 8.0)	115.7	6.58 (d, 8.0)	115.5	6.58 (d, 7.3)	115.4	6.48 (d, 7.3)	115.2
7’	–	156.7	–	156.7	–	156.3	–	156.4
3’-OH	–	–	–	–	–	–	–	–
7’-OH	–	–	–	–	–	–	–	–
-NH	6.10 (br s)	–	6.14 (br s)	–	6.88 (br s)	–	6.74 (br s)	–

[a, b] Overlapping signals; [c] Overlapped with solvent signal; [d] The ratio of *Exo*-enolic form A and B of **1** is approximately 5:1 in $CDCl_3$

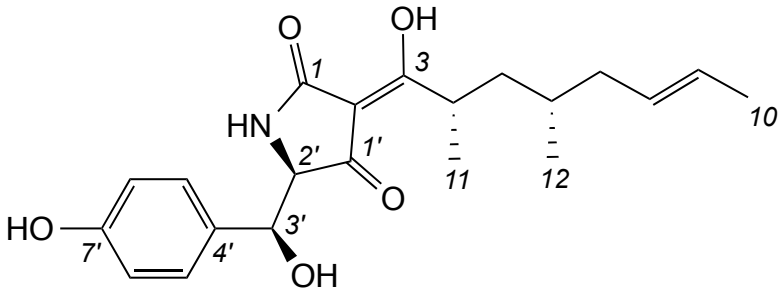

Table S5. NMR (600 MHz, DMSO-d_6) data for chaunolidine A (**2**)

Pos.	δ_H (mult., J (Hz))	δ_C	COSY	HMBC (^{1}H to ^{13}C)
1	–	176.4	–	–
2	–	101.1	–	–
3	–	190.6	–	–
4	3.63 (m)[c]	33.2	5a, 5b, 11	–
5a	1.68 (m)	39.8[d]	4, 5b, 6	4, 6, 12
5b	1.11 (m)[b]		4, 5a, 6	3, 6, 12
6	1.29 (m)	30.7	5a, 5b, 7a, 7b, 12	5, 7
7a	1.91 (m)	39.9[d]	6, 7b, 8	5, 6, 8, 9, 12
7b	1.77 (m)		6, 7a, 8	5, 6, 8, 9, 12
8	5.36 (m)[a]	129.4	7a, 7b, 9	7, 9, 10
9	5.38 (m)[a]	125.9	8, 10	7, 8, 10
10	1.62 (d, 5.0)	17.8	9	8, 9
11	1.08 (d, 6.7)[b]	18.1	4	3, 4, 5
12	0.80 (d, 6.6)	19.3	6	5, 6, 7
1’	–	193.4	–	–
2’	3.95 (br s)	67.8	3’, -NH	1, 1’
3’	4.82 (br s)	71.1	2’, 5’/9’, 3’-OH	5’/9’
4’	–	132.1	–	–
5’/9’	7.14 (d, 8.4)	127.3	3’, 6’/8’	3’, 5’/9’, 6’/8’, 7’
6’/8’	6.69 (d, 8.4)	114.7	5’/9’	4’, 5’/9’, 6’/8’, 7’
7’	–	156.5	–	–
3’-OH	5.41 (m)[a]	–	3’	–
7’-OH	9.26 (s)	–	–	6’/8’, 7’
-NH	8.59 (br s)	–	2’	1’

[a, b] Overlapping signals; [c] Overlapped with residual H_2O signal; [d] Overlapped with residual DMSO signal

Table S6. NMR (600 MHz, $CDCl_3$) data for chaunolidine A (**2**)

Pos.	chaunolidine A (**2**)—*exo*-enolic form A (major)[d]	
	δ_H (mult., *J* (Hz))	δ_C
1	–	176.2
2	–	101.6
3	–	193.0
4	3.78 (m)	34.1
5a	1.20 (m)[b]	40.5[c]
5b	1.17 (m)[b]	
6	1.39 (m)	31.4
7a	1.96 (m)	40.6[c]
7b	1.81 (m)	
8	5.36 (m)[a]	129.5
9	5.40 (m)[a]	126.6
10	1.66 (d, 5.9)	18.1
11	1.19 (d, 6.9)[b]	18.6
12	0.87 (d, 6.5)	19.6
1’	–	193.4
2’	3.97 (d, 2.0)	67.2
3’	5.17 (br s)	72.1
4’	–	132.0
5’/9’	7.23 (d, 7.7)	127.2
6’/8’	6.85 (d, 7.7)	115.9
7’	–	155.9
3’-OH	–	–
7’-OH	–	–
-NH	5.65 (br s)	–

[a, b, c] Overlapping signals;
[d] The ratio of *Exo*-enolic form A and B of **2** is approximately 8:1 in $CDCl_3$, which led to the very weak NMR signals for the minor *Exo*-enolic form B. Therefore, only the NMR data for *Exo*-enolic form A of **2** is listed in the table.

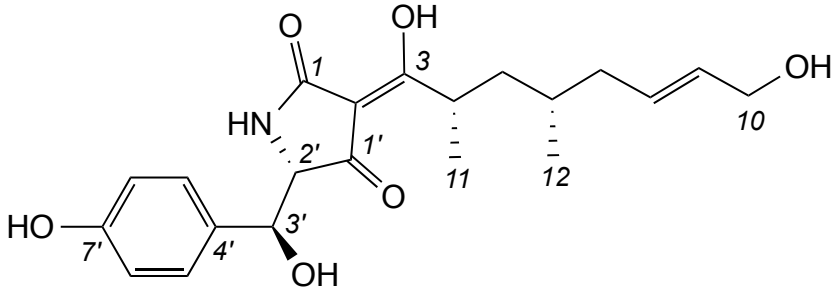

Table S7. NMR (600 MHz, DMSO-d_6) data for chaunolidine B (**3**)

Pos.	δ_H (mult., J (Hz))	δ_C	COSY	HMBC (^{1}H to ^{13}C)
1	–	176.0	–	–
2	–	100.5	–	–
3	–	191.5	–	–
4	3.48 (br s)	33.3	5a, 5b, 11	–
5a	1.62 (m)	39.4[b]	4, 5b, 6	4, 12
5b	1.06 (m)		4, 5a, 6	3, 4, 6, 12
6	1.28 (m)	30.7	5a, 5b, 7a, 7b, 12	–
7a	1.92 (m)	39.7[b]	6, 7b, 8	5, 6, 8, 9, 12
7b	1.77 (m)		6, 7a, 8	5, 6, 8, 9, 12
8	5.48 (m)[a]	132.1	7a, 7b, 9	7, 9, 10
9	5.47 (m)[a]	127.9	8, 10	7, 8, 10
10	3.85 (br s)	61.4	9	8, 9
11	0.88 (d, 6.5)	18.1	4	3, 4, 5
12	0.78 (d, 6.2)	19.1	6	6, 7
1’	–	192.6	–	–
2’	4.16 (br s)	68.0	3’, -NH	1, 1’, 3’, 4’
3’	4.87 (br s)	72.6	2’, 5’/9’	1’, 4’, 5’/9’
4’	–	129.3	–	–
5’/9’	7.00 (d, 8.2)	128.2	3’, 6’/8’	3’, 5’/9’, 6’/8’, 7’
6’/8’	6.59 (d, 8.2)	114.1	5’/9’	4’, 5’/9’, 6’/8’, 7’
7’	–	156.5	–	–
3’-OH	5.64 (br s)	–	–	–
7’-OH	9.23 (s)	–	–	6’/8’, 7’
-NH	9.15 (br s)	–	2’	2, 1’, 2’

[a] Overlapping signals; [b] Overlapped with residual DMSO signal

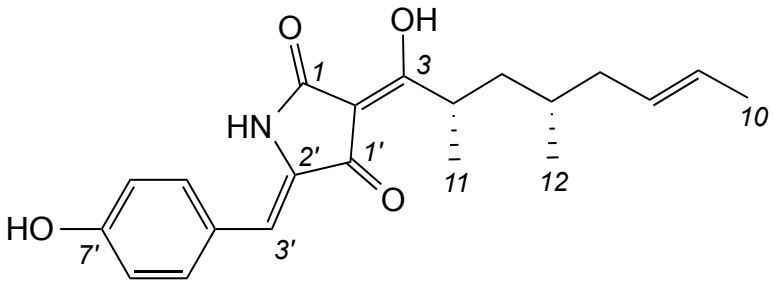

Table S8. NMR (600 MHz, DMSO-d_6) data for chaunolidine C (**4**)

Pos.	δ_H (mult., J (Hz))	δ_C	COSY	HMBC (^{1}H to ^{13}C)
1	–	–[f]	–	–
2	–	–[f]	–	–
3	–	199.2[e]	–	–
4	3.82 (m)	35.9[e]	5a, 5b, 11	5, 11
5a	1.75 (m)[b]	39.8[d]	4, 5b, 6	6, 7, 11, 12
5b	1.14 (m)[c]		4, 5a, 6	4, 7
6	1.36 (m)	30.8	5a, 5b, 7a, 7b, 12	5, 7, 8, 12
7a	1.94 (m)	39.9[d]	6, 8	5, 6, 8, 9, 12
7b	1.78 (m)[b]		6, 8	5, 6, 8, 9, 12
8	5.36 (m)[a]	129.4	7a, 7b, 9	7, 9, 10
9	5.37 (m)[a]	125.9	8, 10	7, 8, 10
10	1.60 (d, 4.2)	17.8	9	8, 9
11	1.12 (d, 6.2)[c]	18.0	4	3, 5
12	0.83 (d, 6.6)	19.3	6	5, 6, 7
1’	–	181.1[e]	–	–
2’	–	–[f]	–	–
3’	6.45 (s)	110.2[e]	–	1’, 5’/9’
4’	–	123.9	–	–
5’/9’	7.52 (d, 8.6)	131.8	6’/8’	3’, 5’/9’, 6’/8’, 7’
6’/8’	6.79 (d, 8.6)	115.8	5’/9’	4’, 5’/9’, 6’/8’, 7’
7’	–	158.3	–	–
7’-OH	9.92 (br s)	–	–	–

[a, b, c] Overlapping signals; [d] Overlapped with residual DMSO signal; [e] Assignments supported by HSQC and HMBC; [f] Carbon signals are weak or broad that cannot be seen in ^{13}C NMR spectrum

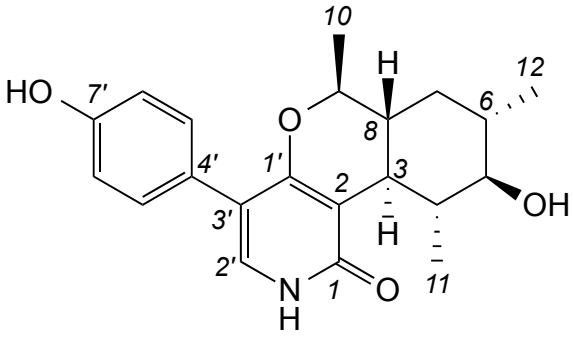

Table S9. NMR (600 MHz, DMSO-d_6) data for chaunolidone A (**5**)

Pos.	δ_H (mult., J (Hz))	δ_C	COSY	HMBC (^{1}H to ^{13}C)	ROESY
1	–	162.6	–	–	–
2	–	111.6	–	–	–
3	2.62 (dd, 10.5, 10.3)	36.1	4, 8	1, 2, 4, 7, 8, 1’	5, 9, 11
4	1.72 (m)	44.3	3, 5, 11	3, 8, 11	6, 7β, 8
5	3.38 (m)[c]	74.7	4, 6	3, 7	3, 12
6	1.60 (m)	37.2	5, 7α, 7β, 12	–	4, 8
7α	1.16 (m)[b]	30.6	6, 7β, 8	5, 6, 12	9
7β	1.40 (m)[a]		6, 7α, 8	3, 9	4, 10
8	1.37 (m)[a]	48.9	3, 7α, 7β, 9	3, 4, 7, 9	4, 6, 10
9	3.66 (m)	77.7	8, 10	3, 8, 1’	3, 7α
10	1.19 (d, 6.2)[b]	18.9	9	8, 9	7β, 8
11	1.10 (d, 6.9)	19.5	4	3, 4, 5	3
12	0.93 (d, 6.7)	18.6	6	5, 6, 7	5
1’	–	162.5	–	–	–
2’	6.99 (s)	130.1	–	1’, 3’, 4’	5’/9’
3’	–	113.1	–	–	–
4’	–	125.1	–	–	–
5’/9’	7.17 (d, 8.5)	129.9	6’/8’	3’, 5’/9’, 6’/8’, 7’	2’
6’/8’	6.72 (d, 8.5)	114.8	5’/9’	4’, 5’/9’, 6’/8’, 7’	–
7’	–	156.2	–	–	–
7’-OH	10.93 (br s)	–	–	–	–
-NH	9.37 (br s)	–	–	–	–

[a, b] Overlapping signals; [c] Overlapped with residual H_2O signal

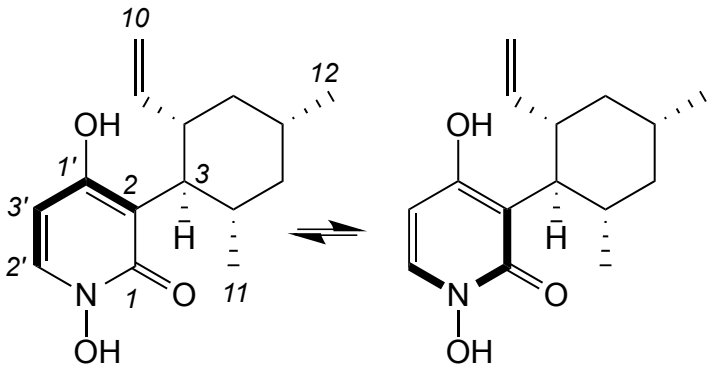

Table S10. NMR (600 MHz, DMSO-d_6) data for pyridoxatin (**6**)

Pos.	Rotamer A (major)[f]		Rotamer B (minor)[f]	
	δ_H (mult., J (Hz))	δ_C	δ_H (mult., J (Hz))	δ_C
1	–	157.8	–	160.3[e]
2	–	112.1	–	112.6
3	2.35 (m)[d]	45.5	2.61 (d, 11.2, 11.2)	45.9
4	3.01 (d, 9.0)	41.5	2.78 (d, 11.0)	42.8
5a	1.67 (m)[a]	41.7	1.68 (m)[a]	41.9
5b	0.84 (m)[b]		0.84 (m)[b]	
6	1.54 (m)	31.4	1.54 (m)	31.5
7a	1.67 (m)[a]	44.2	1.67 (m)[a]	44.3
7b	0.67 (m)[c]		0.68 (m)[c]	
8	2.33 (m)[d]	31.3	2.14 (m)	32.5
9	5.48 (m)	143.5	5.48 (m)	143.5
10a	4.73 (dd, 16.4, 1.6)	112.4	4.76 (d, 16.2, 1.6)	112.5
10b	4.64 (dd, 10.2, 1.6)	–	4.63 (dd, 10.2, 1.6)	–
11	0.62 (d, 5.6)[c]	20.5	0.64 (d, 6.6)[c]	20.5
12	0.89 (d, 6.4)[b]	22.7	0.89 (d, 6.4)[b]	22.6
1’	–	161.2	–	160.3[e]
2’	7.55 (d, 7.6)	131.9	7.50 (d, 7.6)	132.0
3’	5.83 (d, 7.6)	96.3	5.80 (d, 7.6)	97.1
1’-OH	9.97 (br s)	–	9.97 (br s)	–
N-OH	11.06 (br s)	–	11.06 (br s)	–

[a, b, c, d, e] Overlapping signals; [f] The ratio of rotamers A and B of pyridoxatin is approximately 5:3 in DMSO

Table S11. Antimicrobial activities (MIC, μg/mL) of compounds **1–6**

Strain	**1**	**2**	**3**	**4**	**5**	**6**
S. aureus ATCC 25923	>32	>32	>32	8	>32	16
S. epidermidis ATCC 12228	>32	>32	>32	4	>32	>32
B. subtilis ATCC 6633	>32	>32	>32	8	>32	>32
E. coli ATCC 25922	>32	>32	>32	>32	>32	>32
P. aeruginosa ATCC 27853	>32	>32	>32	>32	>32	>32
K. pneumonia ATCC 13883	>32	>32	>32	>32	>32	>32
C. albicans ATCC 90028	>32	>32	>32	>32	>32	>32

Table S12. Cytotoxic activities (IC_{50}, μM) of compounds **1–6**

Cell line	**1**	**2**	**3**	**4**	**5**	**6**
SW620	>30	>30	>30	>30	>30	0.3
NCI-H460	>30	>30	>30	>30	0.09	0.4
KB3-1	>30	>30	>30	>30	>30	0.4

Table S13. HR-ESI(±)-MS analysis of the chelating abilities of compounds **1**, **4**, **5** and **6**

Compound	Metal salt	HRESI(+)MS*	HRESI(–)MS*
F-14329 (**1**)	$FeCl_3$	800 $[TA_2Fe(III)]^+$ (93%)	497 $[TAFe(III) + 2Cl - H]^-$ (46%) 870 $[TA_2Fe(III) + 2Cl]^-$ (100%)
	$FeSO_4$	800 $[TA_2Fe(III)]^+$ (100%)	896 $[TA_2Fe(III) + SO_4]^-$ (100%)
	$CuSO_4$	435 $[TACu(II)]^+$ (17%)	531 $[TACu(II) + SO_4]^-$ (100%)
	$MgSO_4$	769 $[TA_2Mg(II) + H]^+$ (33%)	372 $[TA - H]^-$ (100%)
	$ZnSO_4$	374 $[TA + H]^+$ (100%) 809 $[TA_2Zn(II) + H]^+$ (71%)	372 $[TA - H]^-$ (100%) 532 $[TAZn(II) + SO_4]^-$ (8%)
	$AlCl_3$	771 $[TA_2Al(III)]^+$ (13%)	468 $[TAAl(III) + 2Cl - H]^-$ (38%) 841 $[TA_2Al(III) + 2Cl]^-$ (100%)
Chaunolidine C (**4**)	$FeCl_3$	764 $[TA_2Fe(III)]^+$ (100%)	479 $[TAFe(III) + 2Cl - H]^-$ (100%) 834 $[TA_2Fe(III) + 2Cl]^-$ (75%)
	$FeSO_4$	764 $[TA_2Fe(III)]^+$ (100%)	860 $[TA_2Fe(III) + SO_4]^-$ (100%)
	$CuSO_4$	417 $[TACu(II)]^+$ (100%)	513 $[TACu(II) + SO_4]^-$ (100%)
	$MgSO_4$	356 $[TA + H]^+$ (55%) 733 $[TA_2Mg(II) + H]^+$ (21%)	354 $[TA - H]^-$ (100%)
	$ZnSO_4$	356 $[TA + H]^+$ (100%)	354 $[TA - H]^-$ (100%)
	$AlCl_3$	735 $[TA_2Al(III)]^+$ (11%)	450 $[TAAl(III) + 2Cl - H]^-$ (100%) 769 $[TA_2Al(III) + Cl - H]^-$ (32%)
Chaunolidone A (**5**)	$FeCl_3$	356 $[PD + H]^+$ (100%)	354 $[PD - H]^-$ (9%) 390 $[PD + Cl]^-$ (100%)
	$FeSO_4$	356 $[PD + H]^+$ (100%)	354 $[PD - H]^-$ (100%)
	$CuSO_4$	356 $[PD + H]^+$ (100%)	354 $[PD - H]^-$ (100%)
	$MgSO_4$	356 $[PD + H]^+$ (100%)	354 $[PD - H]^-$ (100%)
	$ZnSO_4$	356 $[PD + H]^+$ (100%)	354 $[PD - H]^-$ (100%)
	$AlCl_3$	356 $[PD + H]^+$ (100%)	354 $[PD - H]^-$ (100%)
Pyridoxatin (**6**)	$FeCl_3$	580 $[PD_2Fe(III)]^+$ (100%)	614 $[PD_2Fe(III) + Cl - H]^-$ (100%)
	$FeSO_4$	580 $[PD_2Fe(III)]^+$ (100%)	676 $[PD_2Fe(III) + SO_4]^-$ (100%)
	$CuSO_4$	325 $[PDCu(II)]^+$ (50%)	421 $[PDCu(II) + SO_4]^-$ (100%)
	$MgSO_4$	264 $[PD + H]^+$ (100%)	262 $[PD - H]^-$ (100%)
	$ZnSO_4$	264 $[PD + H]^+$ (100%)	262 $[PD - H]^-$ (100%)
	$AlCl_3$	551 $[PD_2Al(III)]^+$ (39%)	585 $[PD_2Al(III) + Cl - H]^-$ (100%)

*The ion peak percentage is the ratio of the height of each peak to the base peak that was assigned an abundance of 100 in the chromatogram. (TA stands for tetramic acids, PD stands for pyridinones)

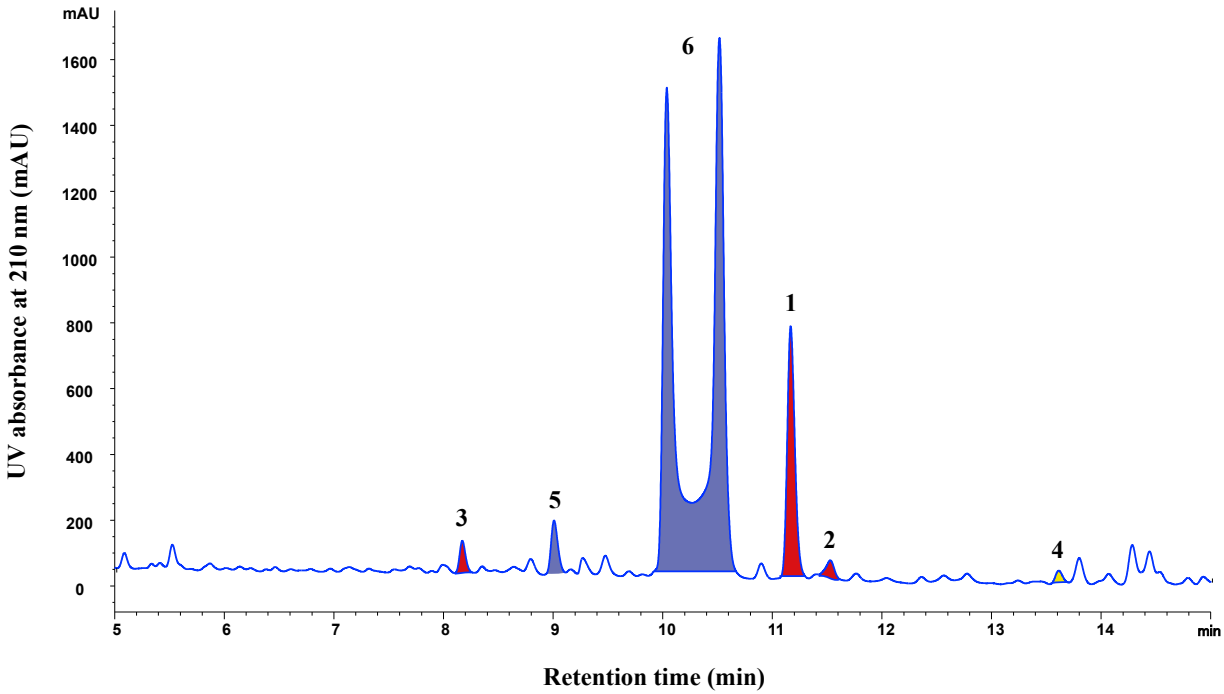

Figure S1. HPLC-DAD profiling (210 nm) of the EtOAc crude extract of fungus *Chaunopycnis* sp. CMB-MF028 and the designation of compounds **1**–**6**

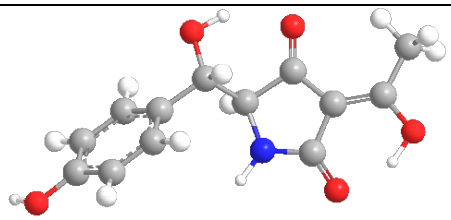	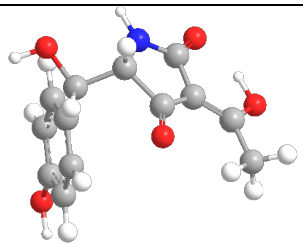
1aC1 (97.31%)	**1aC2** (2.48%)
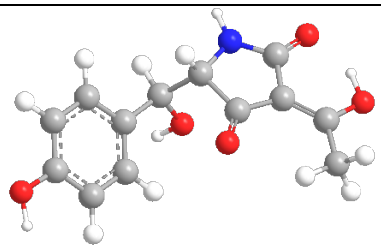	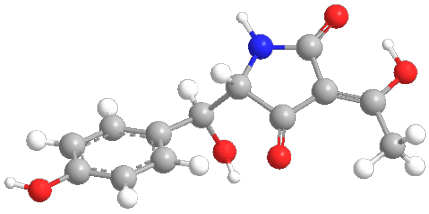
1aC3 (0.17%)	**1aC4** (0.04%)

Figure S2. The optimized four lowest energy conformers (< 6 kcal/mol) of **1a** and their equilibrium populations in MeOH

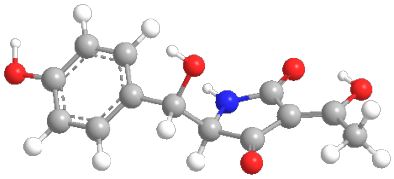	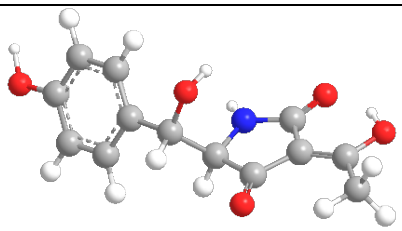
2aC1 (53.93%)	**2aC2** (41.08%)
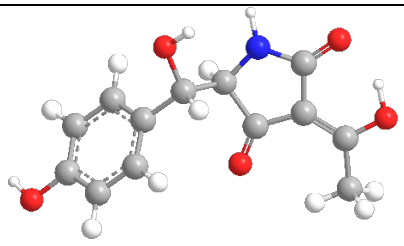	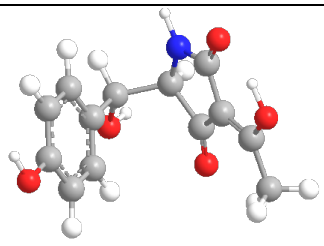
2aC3 (4.37%)	**2aC4** (0.62%)

Figure S3. The optimized four lowest energy conformers (< 6 kcal/mol) of **2a** and their equilibrium populations in MeOH

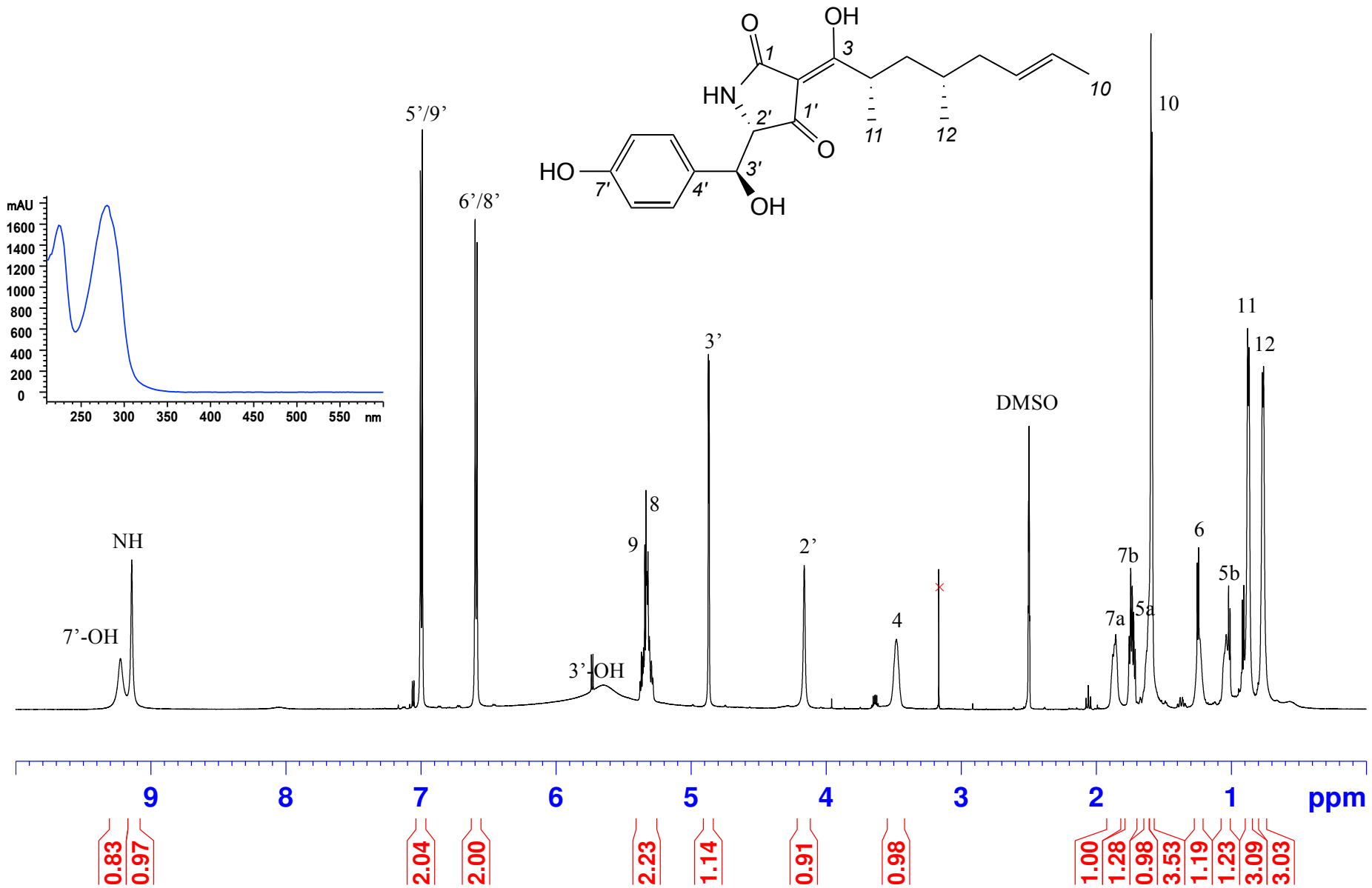

Figure S4. ^{1}H NMR (600 MHz, DMSO-d_6) and UV-vis (inset) spectra of F-14329 (**1**)

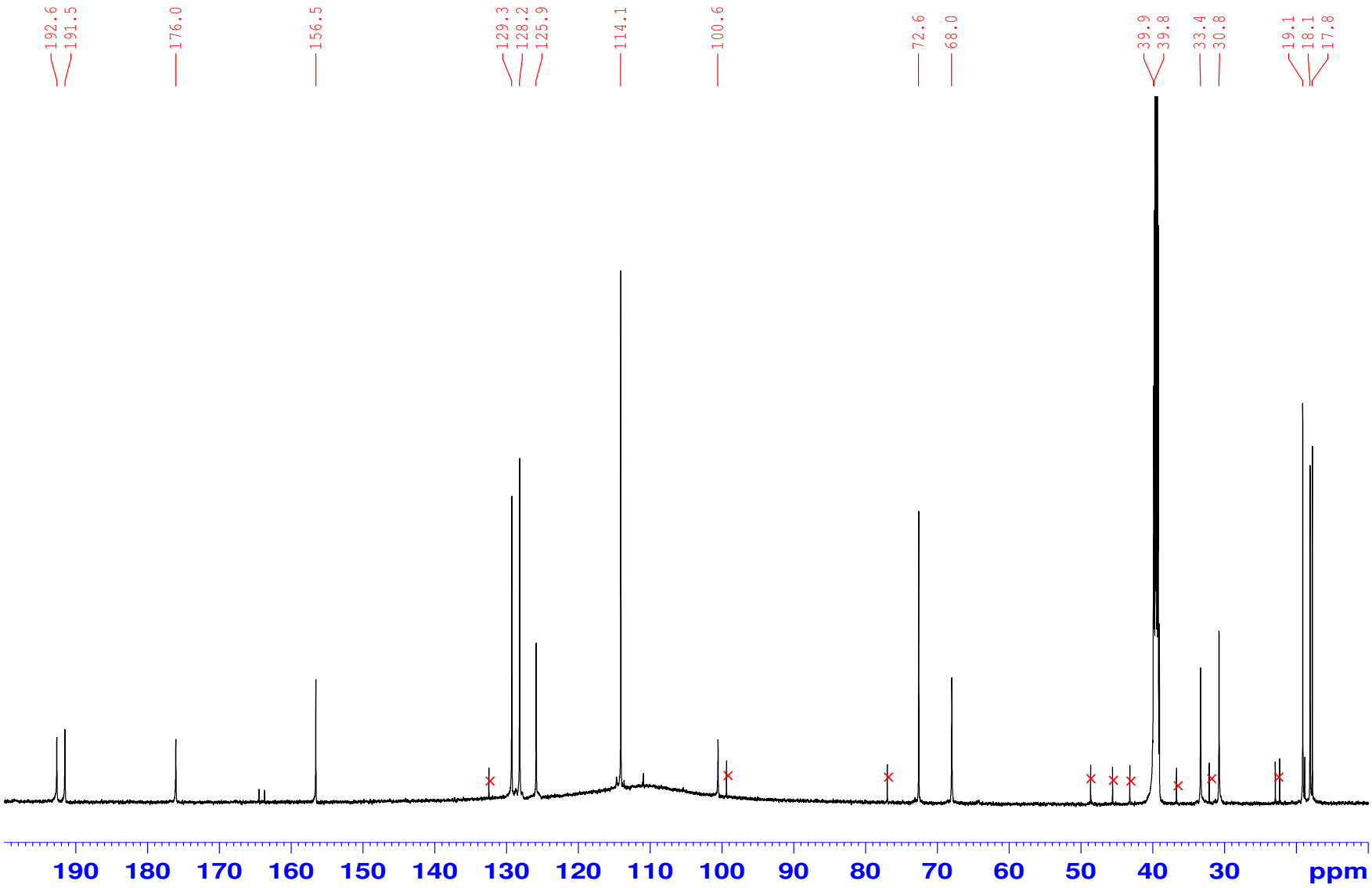

Figure S5. ^{13}C NMR (150 MHz, DMSO-d_6) spectrum of F-14329 (**1**)

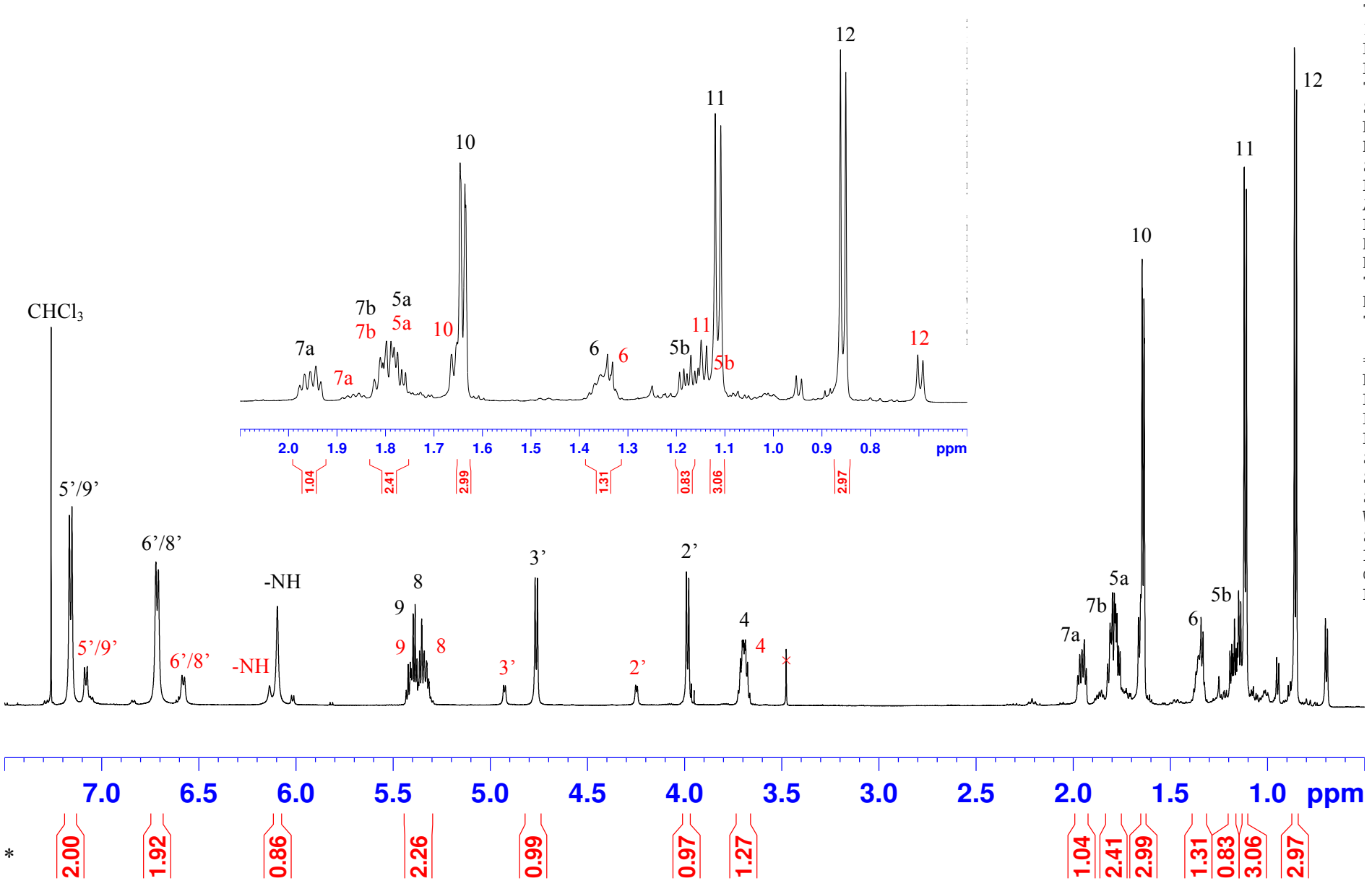

Exo-enolic form A and B of chaunolidine A are labeled in black and red, respectively; only the *Exo*-enolic form A (the major tautomer) is integrated in ^{1}H NMR spectrum.

Figure S6. ^{1}H NMR (600 MHz, $CDCl_3$) spectrum of F-14329 (**1**)

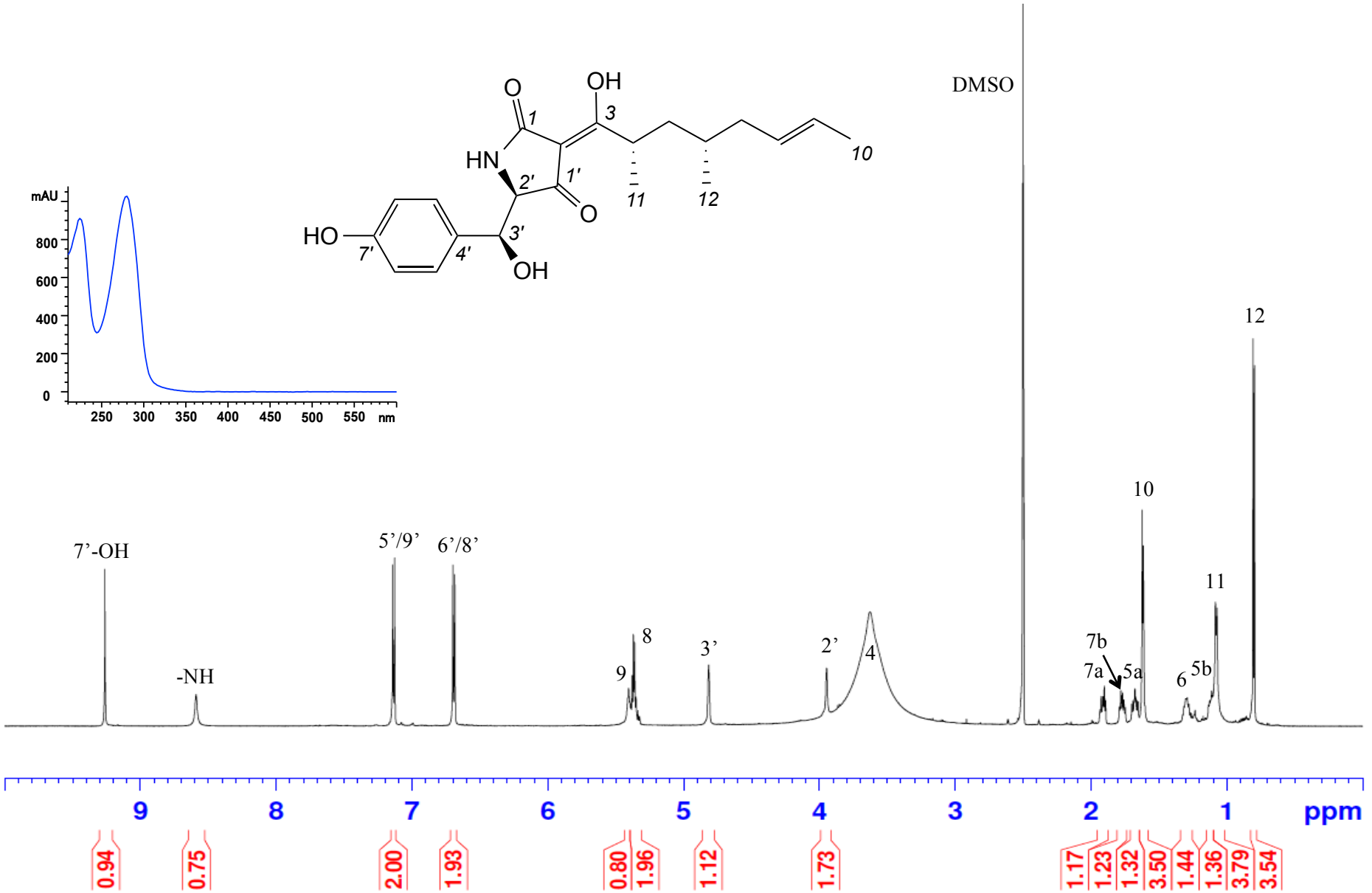

Figure S7. ^{1}H NMR (600 MHz, DMSO-d_6) and UV-vis (inset) spectra of chaunolidine A (**2**)

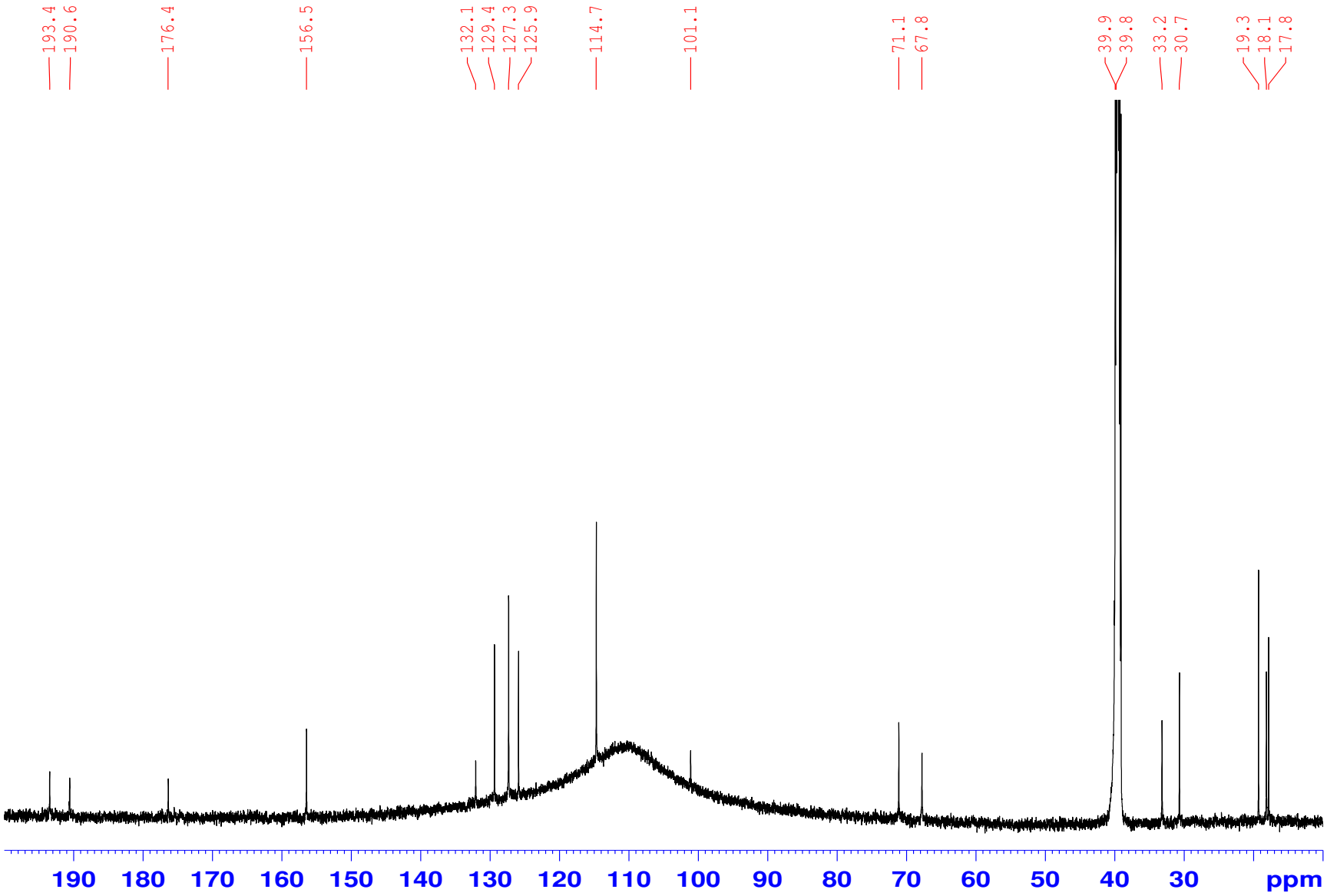

Figure S8. ^{13}C NMR (150 MHz, DMSO-d_6) spectrum of chaunolidine A (**2**)

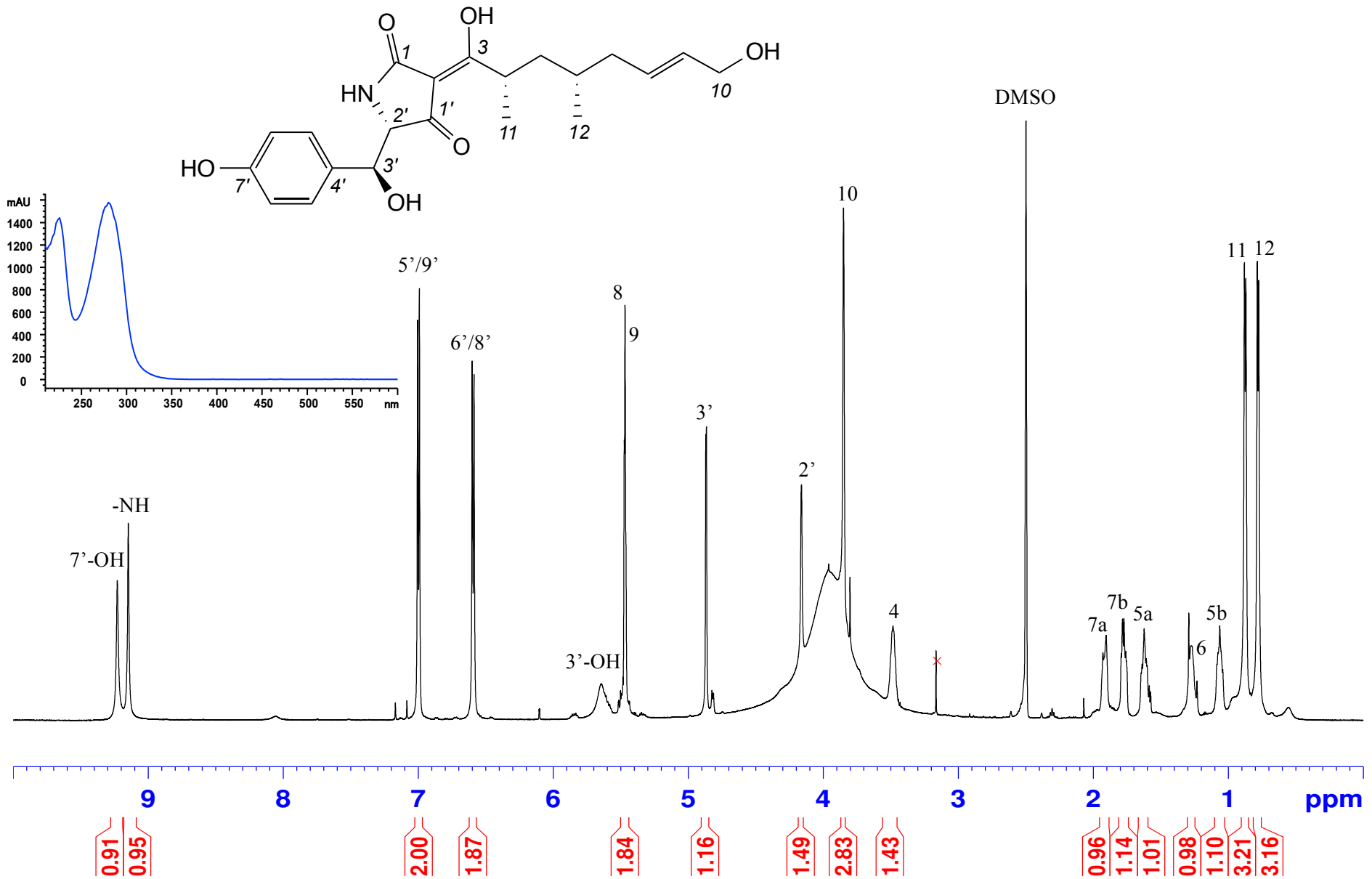

Figure S9. ^{1}H NMR (600 MHz, DMSO-d_6) and UV-vis (inset) spectra of chaunolidine B (**3**)

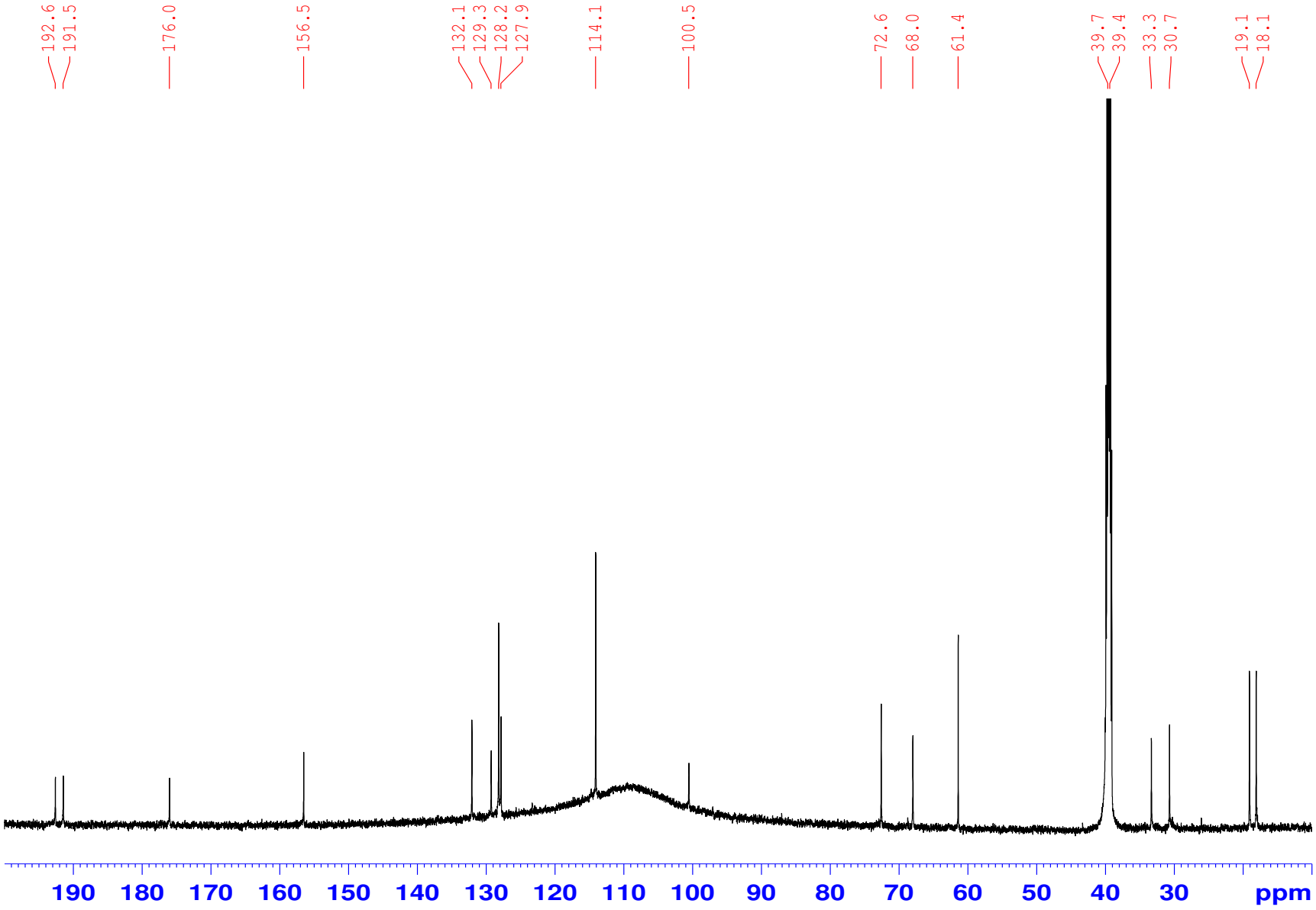

Figure S10. ^{13}C NMR (150 MHz, DMSO-d_6) spectrum of chaunolidine B (**3**)

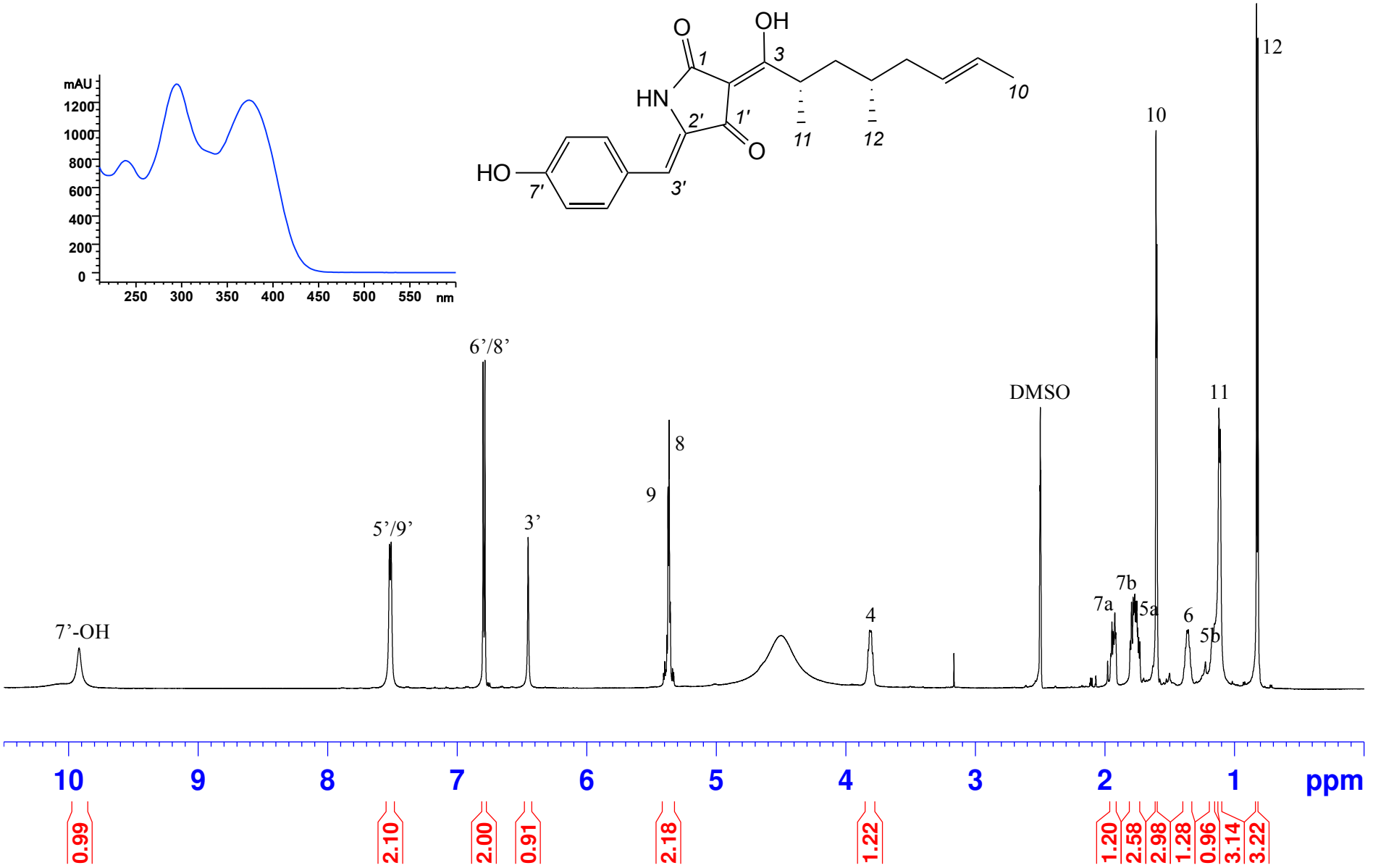

Figure S11. ^{1}H NMR (600 MHz, DMSO-d_6) and UV-vis (inset) spectra of chaunolidine C (**4**)

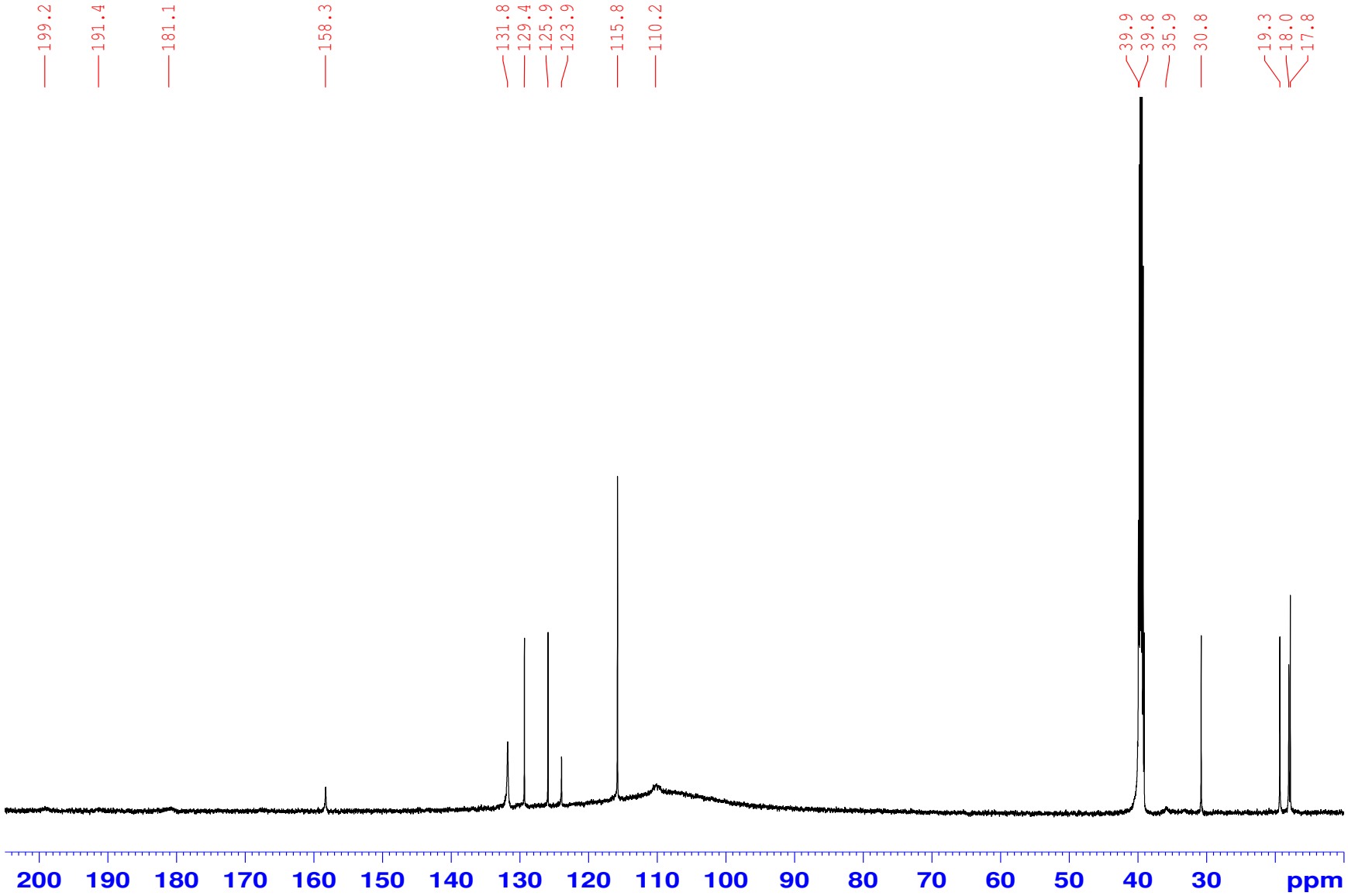

Figure S12. ^{13}C NMR (150 MHz, DMSO-d_6) spectrum of chaunolidine C (**4**)

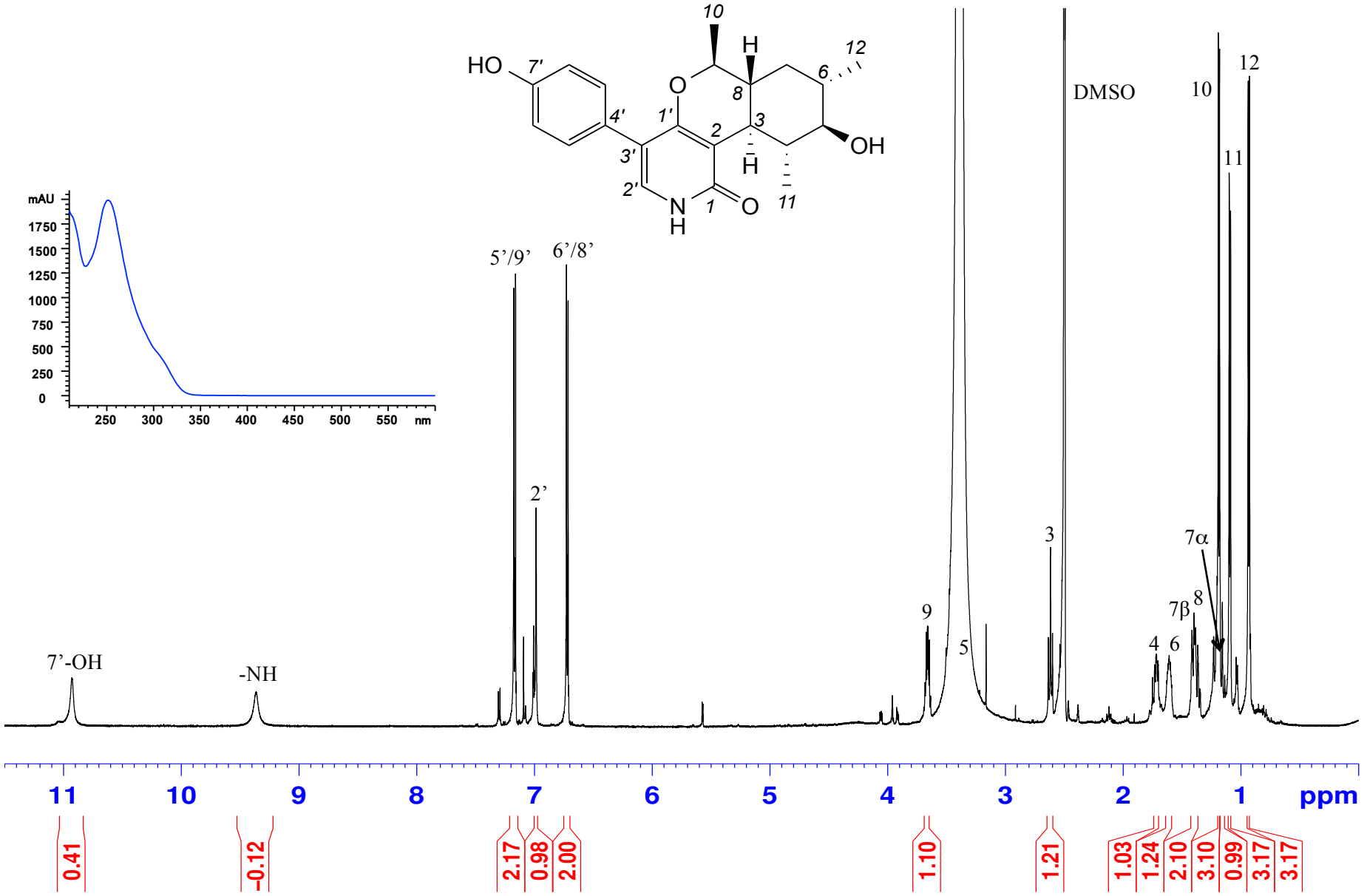

Figure S13. ^{1}H NMR (600 MHz, DMSO-d_6) and UV-vis (inset) spectra of chaunolidone A (**5**)

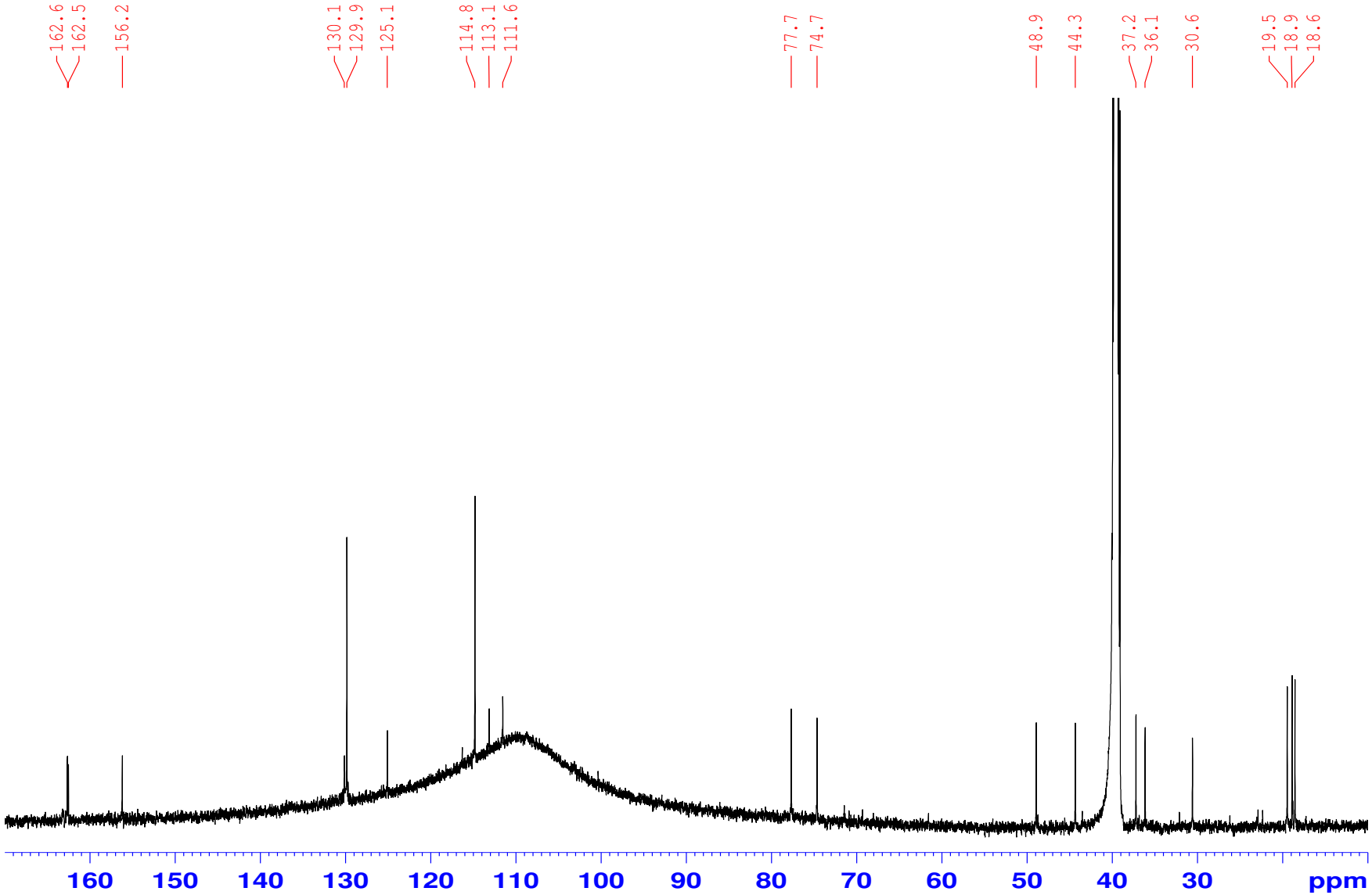

Figure S14. ^{13}C NMR (150 MHz, DMSO-d_6) spectrum of chaunolidone A (**5**)

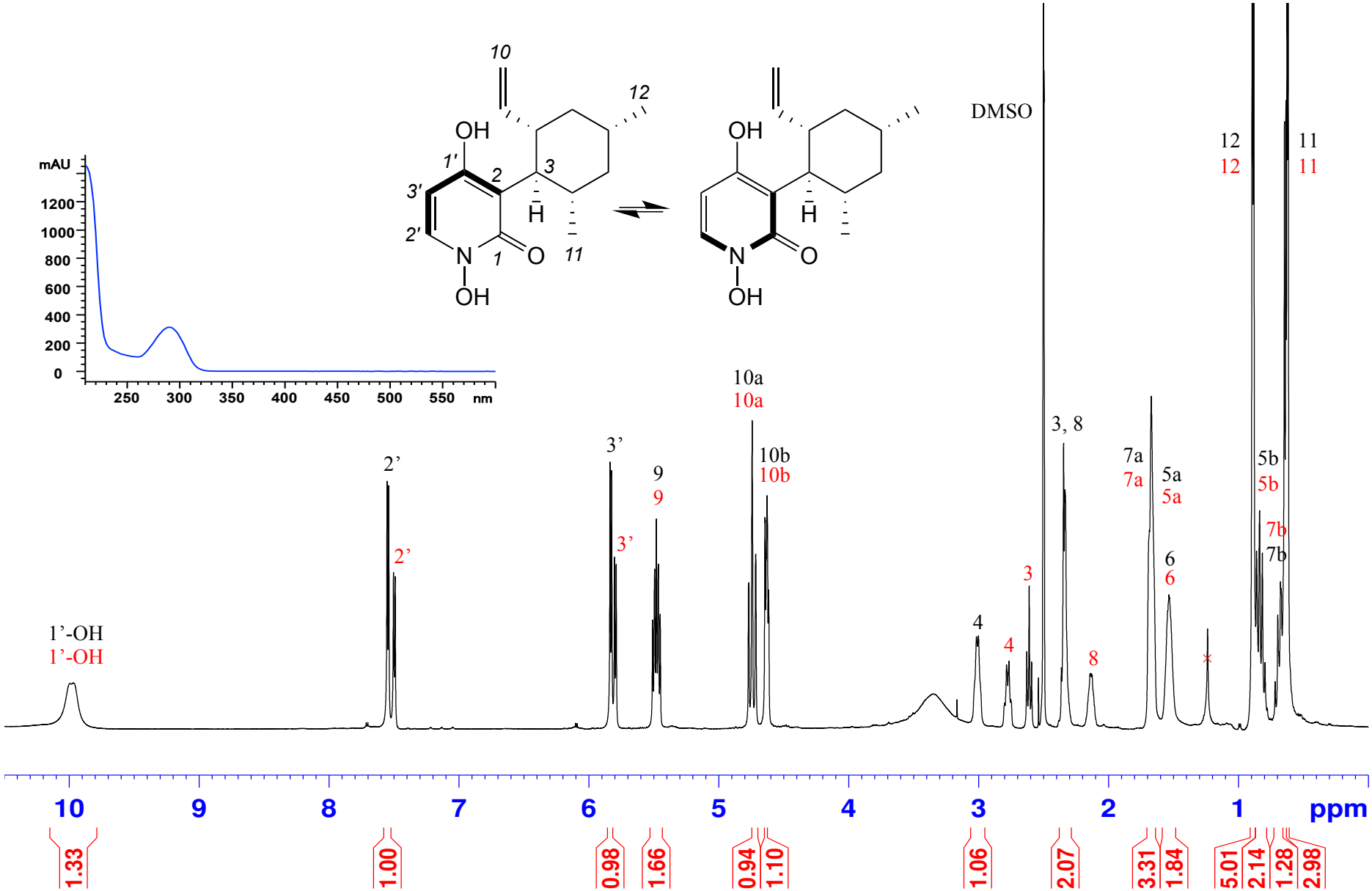

*Major and minor rotamers of pyridoxatin are labeled in black and red, respectively; only the major rotamer is integrated in ^{1}H NMR spectrum.

Figure S15. ^{1}H NMR (600 MHz, DMSO-d_6) and UV-vis (inset) spectra of pyridoxatin (**6**)

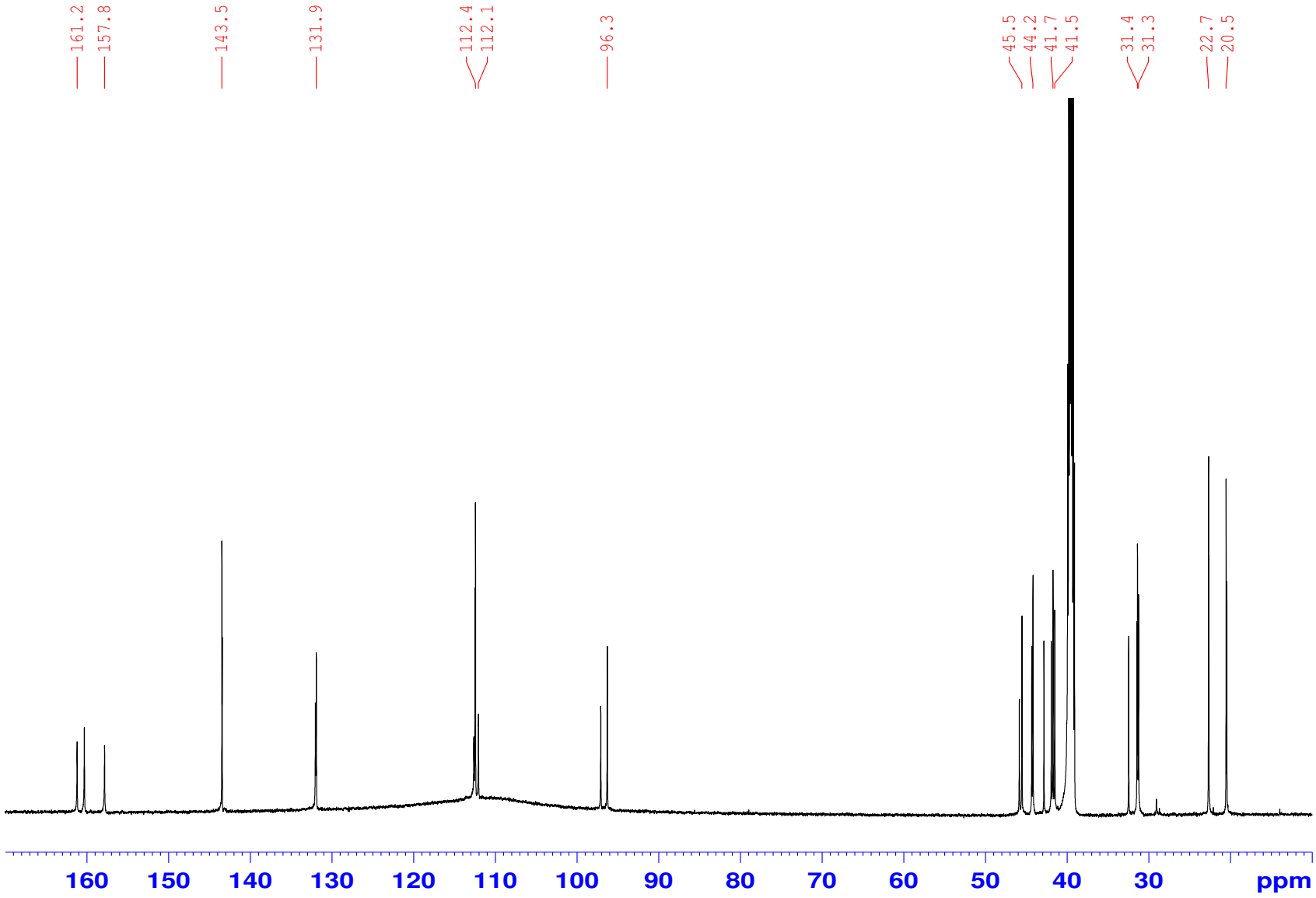

* Only the carbon signals for the major rotamer A of **6** are labeled.

Figure S16. ^{13}C NMR (150 MHz, DMSO-d_6) spectrum of pyridoxatin (**6**)

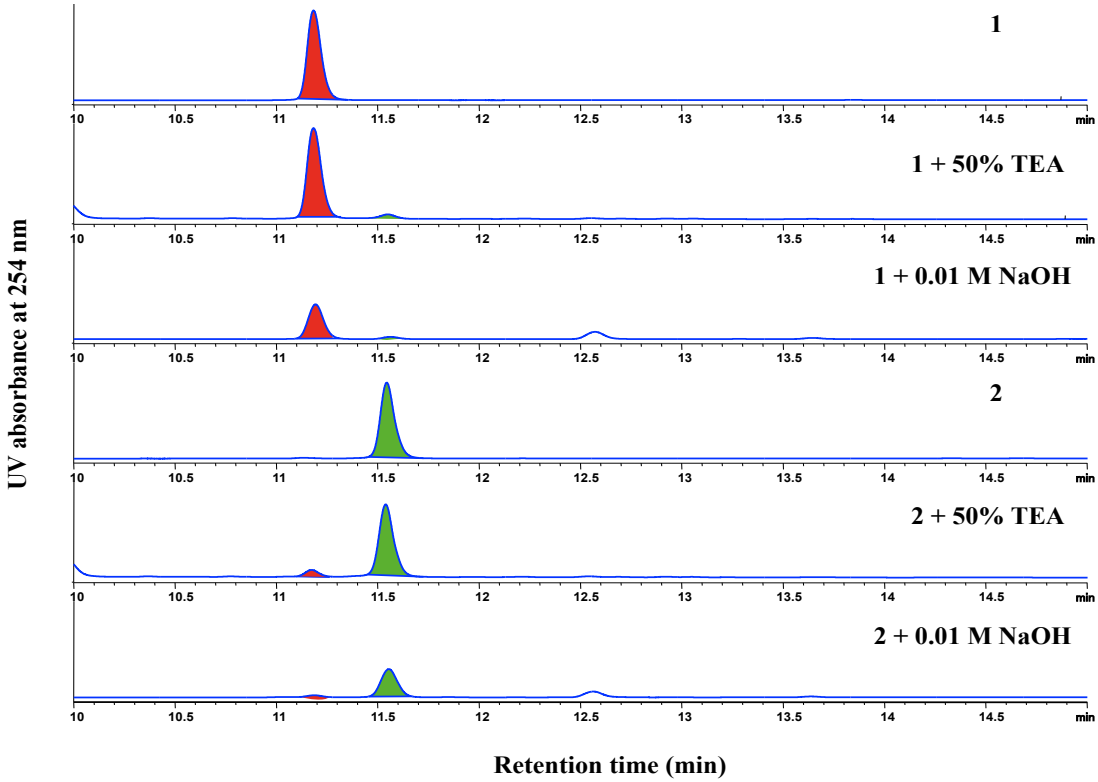

Figure S17. HPLC-DAD profiles of F-14329 (**1**) and chaunolidine A (**2**) after treatment with 50% TEA and 0.01 M NaOH for 12 h (**1** is in red; **2** is in green)

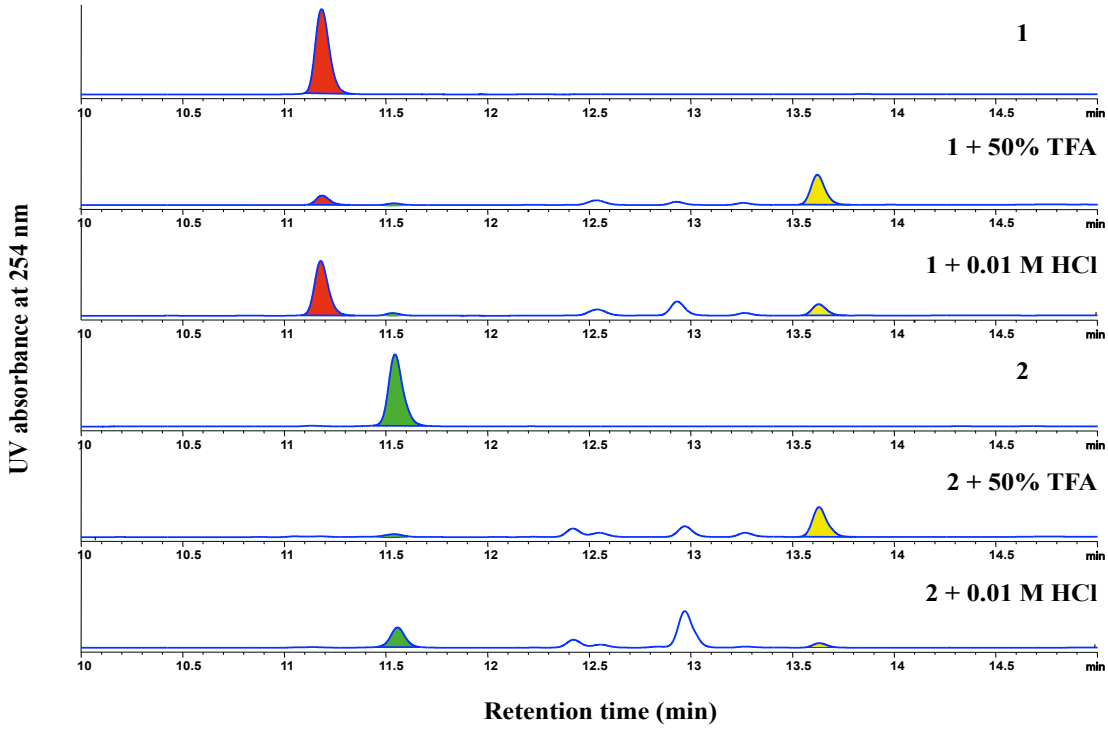

Figure S18. HPLC-DAD profiles of F-14329 (**1**) and chaunolidine A (**2**) after treatment with 50% TFA and 0.01 M HCl for 12 h (**1** is in red; **2** is in green; **4** is in yellow)

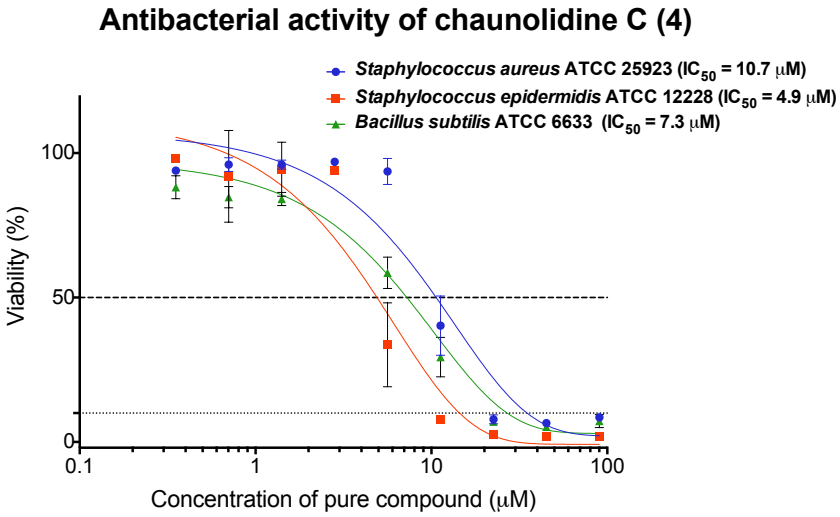

Figure S19. Antibacterial assay (IC_{50}, μM) of chaunolidine C (**4**) against *S. aureus* (ATCC 25923), *S. epidermidis* (ATCC 12228) and *B. subtilis* (ATCC 6633)

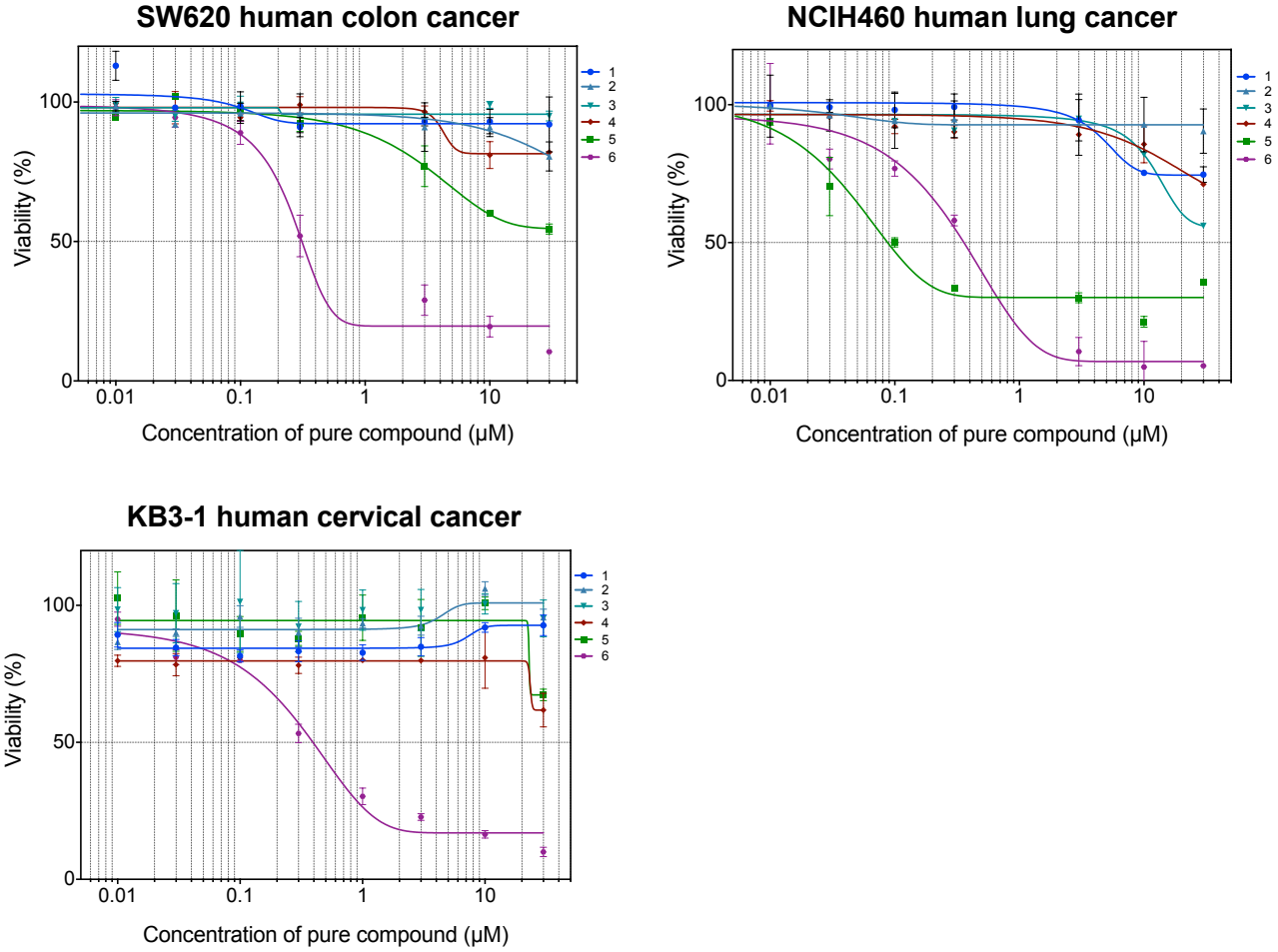

Figure S20. Cytotoxicity assay of compounds **1–6** against SW620, NCIH460 and KB3-1 cell lines

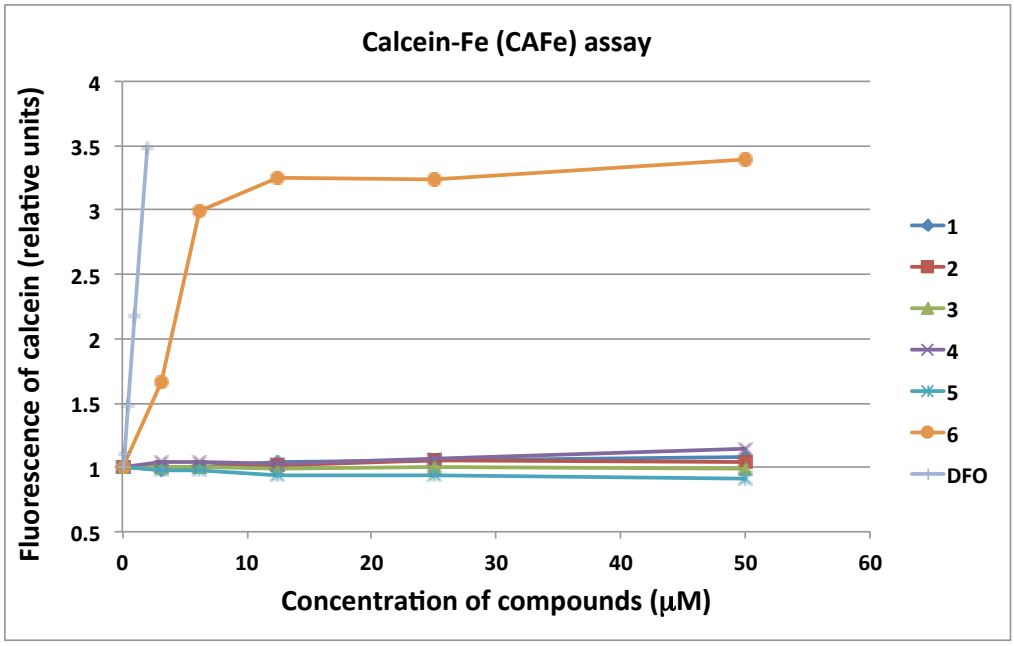

Figure S21. Recovery of calcein fluorescence after CAFe (2 μM) reacted with **1**–**6** for 24 h. (DFO = desferrioxamine as positive control)

4 Single crystal X-ray analysis of chaunolidine C (4)

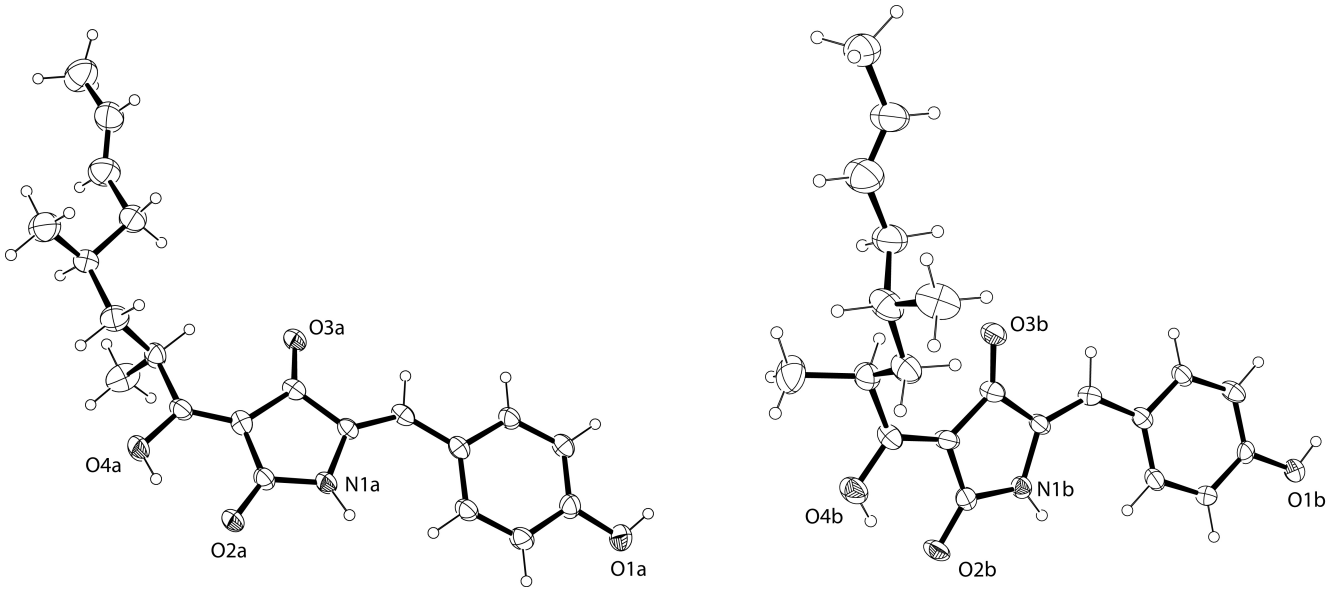

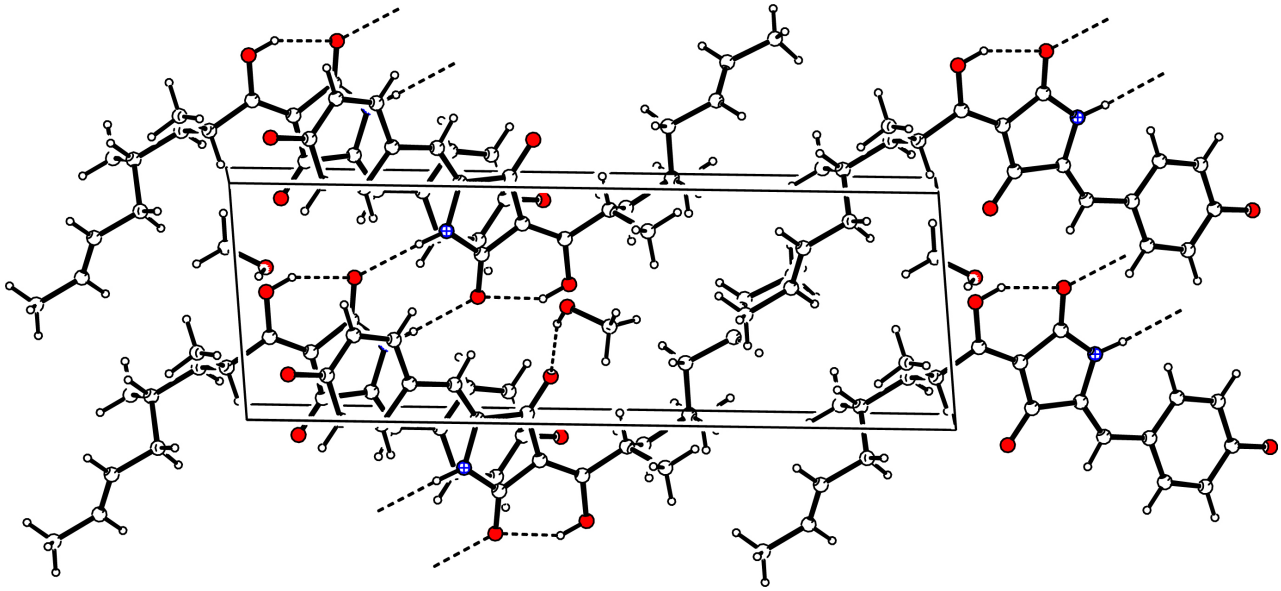

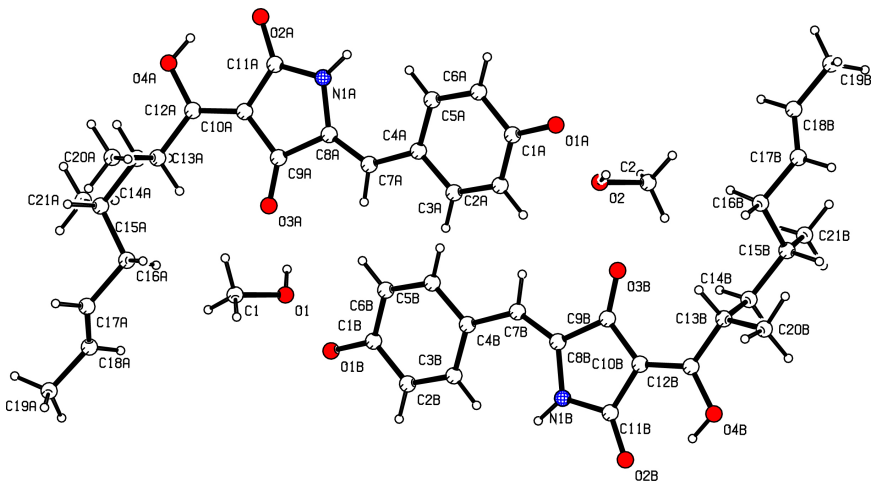

Table 4.1 Crystal data and structure refinement for chaunolidine C (4)

Identification code	1302az7	
Empirical formula	$C_{21}H_{25}NO_4 \bullet CH_3OH$	
Formula weight	387.46	
Temperature	190(2) K	
Wavelength	1.54184 Å	
Crystal system	Triclinic	
Space group	*P* 1	
Unit cell dimensions	a = 6.6012(4) Å	α= 84.197(5)°.
	b = 8.1654(6) Å	β= 84.853(5)°.
	c = 19.8307(13) Å	γ = 85.592(5)°.
Volume	1056.66(12) $Å^3$	
Z	2	
Density (calculated)	1.218 Mg/m^3	
Absorption coefficient	0.698 mm^{-1}	
F(000)	416	
Crystal size	0.2 x 0.1 x 0.1 mm^3	
Theta range for data collection	4.50 to 62.47°.	
Index ranges	-7<=h<=7, -9<=k<=9, -22<=l<=22	
Reflections collected	13470	
Independent reflections	6294 [R(int) = 0.0506]	
Completeness to theta = 62.47°	99.5 %	
Absorption correction	Semi-empirical from equivalents	
Max. and min. transmission	1 and 0.84915	
Refinement method	Full-matrix least-squares on F^2	
Data / restraints / parameters	6294 / 3 / 513	
Goodness-of-fit on F^2	1.031	
Final R indices [I>2sigma(I)]	R1 = 0.0658, wR2 = 0.1664	
R indices (all data)	R1 = 0.0920, wR2 = 0.1858	
Absolute structure parameter	0.1(4)	
Largest diff. peak and hole	0.273 and -0.235 $e.Å^{-3}$	

Table 4.2 Bond lengths [Å] and angles [°] for chaunolidine C (4)

C(1A)-O(1A)	1.365(8)
C(1A)-C(2A)	1.375(9)
C(1A)-C(6A)	1.395(9)
C(2A)-C(3A)	1.368(9)
C(3A)-C(4A)	1.404(8)
C(4A)-C(5A)	1.404(9)
C(4A)-C(7A)	1.437(9)
C(5A)-C(6A)	1.386(9)
C(7A)-C(8A)	1.340(8)
C(8A)-N(1A)	1.422(7)
C(8A)-C(9A)	1.487(8)
C(9A)-O(3A)	1.224(7)
C(9A)-C(10A)	1.467(8)
C(10A)-C(12A)	1.357(8)
C(10A)-C(11A)	1.427(9)
C(11A)-O(2A)	1.253(7)
C(11A)-N(1A)	1.359(8)
C(12A)-O(4A)	1.343(7)
C(12A)-C(13A)	1.490(9)
C(13A)-C(14A)	1.502(9)
C(13A)-C(20A)	1.547(9)
C(14A)-C(15A)	1.544(8)
C(15A)-C(21A)	1.508(9)
C(15A)-C(16A)	1.519(8)
C(16A)-C(17A)	1.525(9)
C(17A)-C(18A)	1.235(10)
C(18A)-C(19A)	1.484(10)
C(1B)-O(1B)	1.339(7)
C(1B)-C(2B)	1.395(9)
C(1B)-C(6B)	1.399(8)
C(2B)-C(3B)	1.393(9)
C(3B)-C(4B)	1.396(8)
C(4B)-C(5B)	1.390(8)
C(4B)-C(7B)	1.467(8)
C(5B)-C(6B)	1.386(9)
C(7B)-C(8B)	1.345(8)

C(8B)-N(1B)	1.410(7)
C(8B)-C(9B)	1.477(9)
C(9B)-O(3B)	1.234(7)
C(9B)-C(10B)	1.434(9)
C(10B)-C(12B)	1.385(9)
C(10B)-C(11B)	1.455(9)
C(11B)-O(2B)	1.248(7)
C(11B)-N(1B)	1.362(8)
C(12B)-O(4B)	1.327(7)
C(12B)-C(13B)	1.479(10)
C(13B)-C(14B)	1.517(9)
C(13B)-C(20B)	1.529(10)
C(14B)-C(15B)	1.546(8)
C(15B)-C(16B)	1.517(9)
C(15B)-C(21B)	1.531(10)
C(16B)-C(17B)	1.495(9)
C(17B)-C(18B)	1.226(10)
C(18B)-C(19B)	1.487(9)
C(1)-O(1)	1.401(9)
C(2)-O(2)	1.395(10)

O(1A)-C(1A)-C(2A)	122.9(5)
O(1A)-C(1A)-C(6A)	117.5(6)
C(2A)-C(1A)-C(6A)	119.5(6)
C(3A)-C(2A)-C(1A)	119.4(6)
C(2A)-C(3A)-C(4A)	123.5(6)
C(3A)-C(4A)-C(5A)	116.1(6)
C(3A)-C(4A)-C(7A)	118.3(6)
C(5A)-C(4A)-C(7A)	125.3(5)
C(6A)-C(5A)-C(4A)	120.9(6)
C(5A)-C(6A)-C(1A)	120.6(6)
C(8A)-C(7A)-C(4A)	132.7(6)
C(7A)-C(8A)-N(1A)	130.2(6)
C(7A)-C(8A)-C(9A)	123.3(5)
N(1A)-C(8A)-C(9A)	106.4(5)
O(3A)-C(9A)-C(10A)	128.5(5)
O(3A)-C(9A)-C(8A)	125.8(5)
C(10A)-C(9A)-C(8A)	105.7(5)

C(12A)-C(10A)-C(11A)	123.2(6)
C(12A)-C(10A)-C(9A)	129.6(6)
C(11A)-C(10A)-C(9A)	107.0(5)
O(2A)-C(11A)-N(1A)	123.4(5)
O(2A)-C(11A)-C(10A)	126.5(6)
N(1A)-C(11A)-C(10A)	110.2(5)
O(4A)-C(12A)-C(10A)	119.7(6)
O(4A)-C(12A)-C(13A)	113.9(6)
C(10A)-C(12A)-C(13A)	126.3(6)
C(12A)-C(13A)-C(14A)	111.0(5)
C(12A)-C(13A)-C(20A)	108.3(6)
C(14A)-C(13A)-C(20A)	113.1(6)
C(13A)-C(14A)-C(15A)	116.3(5)
C(21A)-C(15A)-C(16A)	110.4(5)
C(21A)-C(15A)-C(14A)	109.8(5)
C(16A)-C(15A)-C(14A)	113.1(5)
C(15A)-C(16A)-C(17A)	112.1(5)
C(18A)-C(17A)-C(16A)	129.3(8)
C(17A)-C(18A)-C(19A)	127.1(9)
C(11A)-N(1A)-C(8A)	110.6(5)
O(1B)-C(1B)-C(2B)	118.3(5)
O(1B)-C(1B)-C(6B)	123.0(5)
C(2B)-C(1B)-C(6B)	118.7(5)
C(3B)-C(2B)-C(1B)	120.9(6)
C(2B)-C(3B)-C(4B)	120.8(5)
C(5B)-C(4B)-C(3B)	117.5(6)
C(5B)-C(4B)-C(7B)	118.1(5)
C(3B)-C(4B)-C(7B)	124.3(5)
C(6B)-C(5B)-C(4B)	122.6(6)
C(5B)-C(6B)-C(1B)	119.5(6)
C(8B)-C(7B)-C(4B)	133.5(6)
C(7B)-C(8B)-N(1B)	128.8(6)
C(7B)-C(8B)-C(9B)	123.5(5)
N(1B)-C(8B)-C(9B)	107.7(5)
O(3B)-C(9B)-C(10B)	128.9(5)
O(3B)-C(9B)-C(8B)	125.8(5)
C(10B)-C(9B)-C(8B)	105.3(5)
C(12B)-C(10B)-C(9B)	130.6(5)

C(12B)-C(10B)-C(11B)	121.3(6)
C(9B)-C(10B)-C(11B)	108.2(5)
O(2B)-C(11B)-N(1B)	125.7(5)
O(2B)-C(11B)-C(10B)	126.0(6)
N(1B)-C(11B)-C(10B)	108.3(5)
O(4B)-C(12B)-C(10B)	120.0(6)
O(4B)-C(12B)-C(13B)	116.1(6)
C(10B)-C(12B)-C(13B)	123.8(6)
C(12B)-C(13B)-C(14B)	107.9(6)
C(12B)-C(13B)-C(20B)	112.5(6)
C(14B)-C(13B)-C(20B)	114.2(6)
C(13B)-C(14B)-C(15B)	115.6(6)
C(16B)-C(15B)-C(21B)	110.4(5)
C(16B)-C(15B)-C(14B)	112.7(5)
C(21B)-C(15B)-C(14B)	107.3(6)
C(17B)-C(16B)-C(15B)	113.2(6)
C(18B)-C(17B)-C(16B)	130.8(8)
C(17B)-C(18B)-C(19B)	130.5(7)
C(11B)-N(1B)-C(8B)	110.5(5)

Table 4.3 Hydrogen bonds for chaunolidine C (4) [Å and °]

D-H...A	d(D-H)	d(H...A)	d(D...A)	<(DHA)
N(1A)-H(1A)...O(2B)#1	0.88	2.09	2.884(6)	150.2
O(1A)-H(1A1)...O(2)	0.84	1.89	2.713(7)	167.7
O(4A)-H(4A)...O(2A)	0.84	1.91	2.664(6)	148.0
N(1B)-H(1B)...O(2A)#2	0.88	2.10	2.890(6)	148.4
O(1B)-H(1B1)...O(1)#3	0.84	1.88	2.710(6)	168.2
O(4B)-H(4B)...O(2B)	0.84	1.88	2.636(6)	149.3
O(1)-H(1)...O(3A)	0.84	1.92	2.725(6)	161.3

Symmetry transformations used to generate equivalent atoms: #1 x-1,y,z #2 x+1,y,z #3 x-1,y+1,z

References

1 J. Carmichael, W. G. DeGraff, A. F. Gazdar, J. D. Minna and J. B. Mitchell, *Cancer Res.* 1987, **47**, 936.
2 M. M. Baccan, O. Chiarelli-Neto, R. M. Pereira and B. P, Espósito, *J. Inorg. Biochem.* 2012, **107**, 34.
3 T. Nakada, M. Nakajima, H. Kobayashi, M. Takahashi and I. Tanaka, *Jpn. Kokai Tokkyo Koho*, Vol. JP 2007153840 A 20070621, 2007.